Numerical Modelling of Geothermal Energy Piles: Thermo-mechanical Behaviour and Thermal Performance

By

Nanwangzi Wu

A thesis submitted in fulfilment of the requirements for the degree of

Master of Philosophy

Faculty of Engineering and Information Technology

The University of Sydney

2018

Abstract

In recent decades, geothermal energy piles have been widely used as a sustainable resource for heating and cooling buildings. This relatively new technology aims to utilise the fairly constant underground temperature to address environmental issues by reducing carbon emissions and other harmful chemicals, such as Freon, from entering the atmosphere, by providing alternatives to widely used air conditioning. The application of geothermal energy pile also provides beneficial long-term financial returns because of its low electricity consumption. During building construction, it provides advantages for the vendor and developer by saving land, compared to conventional Geothermal Ground Heat Exchangers (GHEs). The piles provide structural and other functional purposes and therefore offer huge potential economic and environmental motivation for this technology to be further developed.

This thesis is based on a numerical approach, the Finite Element Method (FEM), using commercial software ABAQUS to study the performances of geothermal energy piles. Settlement response and thermal performance are two major aspects in the design of geothermal energy piles. Firstly, thermal cyclic loading conditions (heating and cooling the piles) lead to further settlement compared with conventional pile foundations, and its additional settlement may cause structural damage if not considered properly. Secondly, determining the output power of geothermal energy piles is important because grouping the piles may cause spacing effects that would reduce the overall thermal performance.

In Chapter 4, numerical modelling of small-scale geothermal energy pile settlement under cyclic loading was conducted and compared with experimental data. Thirty cooling and heating cycles were applied under constant mechanical loading, corresponding to 0%, 20%, 40% and 60% ultimate pile resistance, representing a real situation for 30 years. The results obtained show an increase of irreversible pile head settlement with the thermal cycles. This highlights

the importance of pile thermal contraction/expansion in pile/soil interaction under thermo-mechanical loading. Moreover, energy efficiency of energy pile grouping was studied in Chapter 5. Single pile thermal performance was investigated and compared with the analytical solution of finite line source. Then, the study was extended to the pile group for further investigation. Different pile centre-to-centre spacings of 1 m and 2 m were studied to determine the influence of spacing. The study of pile groups enables investigation of the best operational techniques to maximise power output for geothermal energy piles.

Table of Contents

List of Figures

List of Tables

École des Ponts
ParisTech

Object : Autorisation letter

Paris, November 20, 2018

To whom it may concern,

With this letter I hereby confirm:

Nanwangzi WU is a co-author of the manuscript *"Long-term thermo-mechanical behaviour of energy pile in clay"*, accepted for publication in Environmental Geotechnics (Article number: ENVGEO-D-17-00106R2), as a part of his M.Phil thesis. Nanwangzi performed numerical simulation, analyzed results and wrote the paper.

Sincerely,

Dr. Anh Minh TANG

Research Director

Ecole des Ponts ParisTech
Laboratoire Navier/Géotechnique (CERMES)
6-8 avenue Blaise Pascal
77455 MARNE-LA-VALLEE
France
Tel: +33.1.64.15.35.63
http://navier.enpc.fr

UNIVERSITÉ PARIS-EST
École nationale des ponts et chaussées
6 et 8 avenue Blaise-Pascal, Cité Descartes
Champs-sur-Marne F-77455 Marne-la-Vallée cedex 2
tél. 33 (0)1 64 15 30 00
fax. 33 (0)1 64 15 34 09
www.enpc.fr

Chapter 1. Introduction

For decades, fossil fuel depletion has been a global topic, with the majority of total energy production coming from non-sustainable resources. As a result, energy prices have risen; however, global warming caused by carbon dioxide emission is a more serious global environmental issue. In civil engineering, how to apply recent technologies into civil construction to address this global issue is challenging. Geothermal energy is considered as a sustainable energy resource that has been studied for years. The utilisation of this energy resource would enhance progress towards a cleaner environment and would be cost-effective for potential end-users.

The usage of geothermal energy starts from a Geothermal Ground Heat Exchangers (GHEs) which is purely a heat exchanger without any structural function. It can be installed vertically or horizontally, hence called a vertical or horizontal GHEs. They can also be subdivided into shallow and deep GHEs. Generally, a deep ground heat exchanger is mainly constructed for electricity generation that extracts heat at over 100 °C, extending by a borehole depth of hundreds of metres. Shallow ground heat exchangers are mainly used for shallow thermal energy foundations in commercial and residential buildings that directly utilise potential thermal energy to reduce usage of air conditioners. This thesis is focused on shallow geothermal energy foundations.

The system used in conventional GHEs requires a relatively large land volume for additional borehole installation, regardless of using horizontal or vertical GHEs. This technology utilises closed-loop heat exchange to transfer heat between the soil body and the overlaying structure (Murphy et al., 2015) by using a relatively constant underground soil temperature potential of approximately 15 °C in most areas (Brandl, 2006). GHE systems are relatively expensive to install, and are therefore not cost-effective for developers' revenue-returns strategies (Park et

al., 2013). Alternatively, in recent decades, geothermal energy piles have been treated as an alternative GHE technique. They combine structural and thermal functions for a building to reduce energy consumption. Energy piles provide a cost and energy efficient solution to the installation and application of GHEs by additionally providing structural foundations.

Geothermal energy piles are designed and constructed with a dual function. In non-operating time, they act as normal structural piles to ensure settlement of the building is within the safety and serviceability requirements; and in operating time, they have the additional duty of heating and cooling the building as air conditioning. Figure 1.1 (Laloui et al., 2006) illustrates the working principles of geothermal piles. Normally, a heat pump and condenser are installed between the piles and the overlaying structure, acting as air conditioning. According to Laloui et al., (2006), new buildings can save up to 50% total energy if this technology is properly applied.

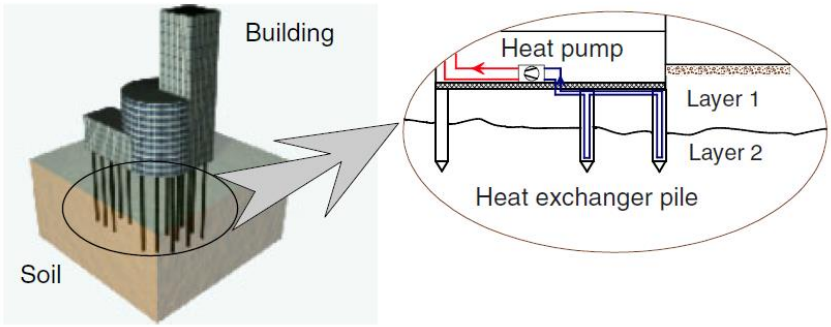

Figure 1.1Illustration of the geothermal energy pile system (Laloui et al., 2006)

Compared to a conventional structural pile, the geothermal energy pile is normally designed with a water circulation tube in the inner core of the pile. Generally, water pipe configurations are U-, W- or helix-shaped. The purpose of this configuration is to ensure thermal exchange efficiency, as shown in Figure 1.2 (Carotenuto et al., 2017). A system of heat exchange pipes is constructed inside such piles to allow the exchange of thermal energy between the ground

and the building via the water circulating in the pipes. This system combined with a heat pump enables heat to be extracted from the soil in winter and re-injected back into the soil in summer.

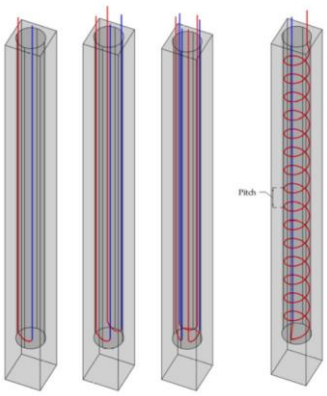

Figure 1.2 Different water pipe configurations for geothermal energy piles (Carotenuto et al., 2017)

In recent years, studies of geothermal energy piles have focused on long-term settlement behaviour, thermal cyclic behaviour and pile thermal performance. In order to industrialise this technology, many researchers use in-situ laboratory experiments and numerical simulations to investigate the thermal and mechanical behaviour of geothermal energy piles (Baycan et al., 2013; Bourne-Webb et al., 2009; Di Donna et al., 2016; Laloui et al., 2006; Nguyen et al., 2017; Stewart & McCartney, 2013; Yavari et al., 2014a). Based on previous research, this study aims to gain a better understanding of the mechanical behaviour of geothermal energy piles and advance regulation of the relevant requirements for geothermal energy pile application.

The structure of the thesis reads as follows. A detailed review on recent studies is given in Chapter 2 covering both experimental and numerical approaches on energy pile performances. The finite element model and methodology adopted in this thesis are then discussed in Chapter 3. Thermo-mechanical behaviour of geothermal energy piles under cyclic loading is reported in Chapter 4, and a thermal performance study for pile grouping is presented in Chapter 5. Finally, the conclusion and future works are discussed in Chapter 6.

Chapter 2. Literature Review

In this chapter, related works for geothermal energy piles are reviewed in the aspects of pile structural mechanics and thermal performance. From a pile foundation design perspective, additional settlement caused by temperature cycles is a challenge for safety and serviceability of energy pile foundations. In Heating Ventilation and Air conditioning (HVAC) engineering, heat transfer performance design is important if the application of geothermal energy piles is to become a reality. In fact, several applications have already been constructed in Europe, such as the Frankfurt Main Tower and Dock E at Zurich Airport. However, the mechanics has not been fully understood, therefore some applications of geothermal energy piles have been overdesigned for safety reasons (Laloui et al., 2006). As such, experimental and numerical studies are still ongoing in research laboratories worldwide.

2.1 Mechanical responses

The mechanics of geothermal energy piles is generally studied by conventional load transfer methods, in-situ testing, laboratory testing and numerical simulation. Instead of bearing actual building loads, in-situ testing provides the conditions of a real construction situation and could provide the most reliable data before actual construction, however, the cost of in-situ testing is relatively high compared with laboratory testing of scaled physical models (Yavari et al., 2014a). To reduce experimental costs, laboratory testing and numerical simulation are performed by many researchers (Bodas Freitas et al., 2013; Bourne-Webb et al., 2009; Di Donna & Laloui, 2015; Laloui et al., 2006; Loria et al., 2015; Saggu & Chakraborty, 2015). Some studies investigated the mechanical behaviour of energy piles subjected to numerous thermal cycles, which represents seasonal pile temperature variations (Di Donna & Laloui, 2015; Ng et al., 2016; Ng et al., 2014; Nguyen et al., 2017; Olgun et al., 2015; Pasten & Santamarina, 2014; Saggu & Chakraborty, 2015; Suryatriyastuti et al., 2014; Vieira &

Maranha, 2016). The mechanical response of geothermal energy piles in literature is reviewed here and identifies the general ideas of how to design a geothermal energy pile from a geotechnical engineering perspective.

2.1.1 Load transfer method

The conventional load transfer method is the simplest way to estimate energy pile mechanisms. Suryatriyastuti et al., (2014) used this method, combined with additional mechanisms for predicting degradation behaviour of the pile-soil interface under thermal cycles, and investigated the behaviour of free- and restraint-head piles in loose sand. The results show a ratcheting of pile head settlement under a constant working load and a decrease in pile head force for the restraint-head pile after 12 thermal cycles. Pasten and Santamarina (2014) developed a modified one-dimensional load transfer model to predict the displacement of pile elements. The results show that the axial force changes mainly in the middle of the pile length when the pile works under a heating phase. But in a cooling phase, the axial force changes are negligible. Besides, the irreversible settlement of a pile reaches a plateau after several thermal cycles. Mimouni and Laloui (2014) emphasised three different pile type mechanisms: floating pile, semi-floating pile and end-bearing pile. For a floating pile, the head reaction and shaft friction below the null point increase with temperature, while the shaft friction along the area above the null point decreases. For a semi-floating pile, base compression and shaft friction below the null point of the pile increases with temperature and shaft friction above the null point of the pile decreases. The head reaction increases when the pile head heaves with temperature. The sharp transition in shaft friction from positive to negative temperature variations is observed in the semi-floating pile compared to the floating pile. Because an end-bearing pile has no shaft friction, the head load is transferred to the pile toe at any time. Since many cases of energy piles have been overdesigned, it is suggested that overdesigned piles do

not have a positive influence from a serviceability standpoint and can even have a negative impact whilst also increasing construction costs.

2.1.2 In-situ testing

An in-situ test pile was constructed and tested at the Swiss Federal Institute of Technology in Lausanne (EPFL) as a part of the new building structure (Laloui et al., 2006). The thermal and mechanical behaviour was investigated with an 88 cm diameter, 25.8 m long pile located at the side of a building (100 m height and 30 m width). Seven thermal mechanical tests were carried out, with one thermal cycle in each test. The experimental results show that the mechanical stress is large on the top of the pile and then decreases along the depth, whilst the pile toe carries almost no load. However, the thermal stress appears to act in the opposite way, where the thermal stress is smaller on the top and increases along the pile depth when temperature increases; 1°C increments induce 100 kN vertical force in this case. Numerical simulation was also performed in this case study and will be reviewed in the following section. Figure 2.1 shows an on-site picture of the pile location, the ground soil property profile in this in-situ experiment.

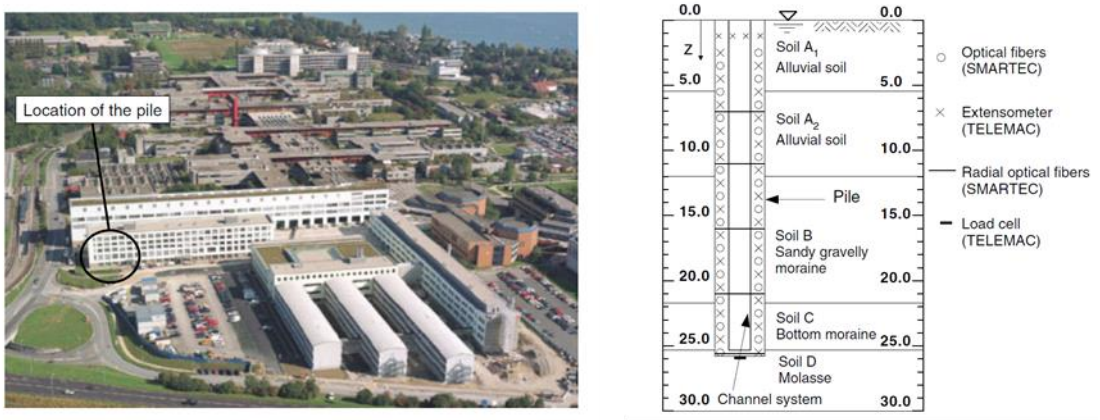

Figure 2.1 (a) On-site picture of the pile location and (b) ground soil property profile after the experiment at EPFL (Laloui et al., 2006)

Another in-situ experiment was conducted at Lambeth College, London after the EPFL pile testing (Bourne-Webb et al., 2009). The upper 5 m of the shaft was cased through the artificial ground and terrace deposits, with a shaft diameter of about 610 mm. Below the casing, the pile shaft was constructed with a 550 mm diameter and 23 m total depth. One cooling test and one heating test were carried out before the failure test. It is suggested that cooling of the pile caused tensile forces to occur near the pile toe, whilst reverse effects appeared when the pile experienced heating. Because of different restraint conditions, the EPFL testing pile had strong constraints at both ends, whereas the Lambeth College testing pile was imperfectly restrained. The uniform load increase in the EPFL testing pile was not repeated in the Lambeth College testing pile cases.

Similar phenomena were reported in other literatures (Akrouch et al., 2014; Murphy et al., 2015). Even when constructing the piles together in one building, the restraint condition difference results in a 1 MPa stress change between the corner pile and the centre pile in the grade beam, and a linear strain increment is experienced with temperature at each depth when the thermal load is applied. Since subsequent thermally induced settlement is relatively insignificant after one thermal cycle application, the authors declared no structural damage to the building when using this technology. Thermal performance has also been studied (Murphy et al., 2015) and it will be discussed in the following section. Akrouch et al., (2014) built a full-scale testing pile located at the Texas A&M University, Riverside Campus. Five different mechanical loads were applied, with a thermal load in each region that had high plasticity clay. Such clay may have had more time-dependant displacement since the creep rate would rise with a temperature rise. It was suggested that under long-term behaviour of the energy pile (i.e., 50 years), more attention would be needed in terms of additional displacement in heating/cooling operation.

2.1.3 Laboratory testing of small-scale and centrifuge models

Laboratory experiments of scaled physical models are an effective method to study the mechanisms of geothermal energy piles. Stewart and McCartney (2013) investigated the influence of thermal cyclic loading performance of a single 533.4 mm long end-bearing pile on unsaturated silt using a centrifuge test to simulate a full-scale energy pile length of 12.8 m (with a scaling factor 24). The temperature change was 19°C and four thermal cycles were applied. The results show that the centrifuge test was in a good agreement with full-scale end-bearing energy foundations, though limitations occurred in the heat transfer process. This may due to different scaling factors relevant to the corresponding mechanical and thermal processes. Further centrifuge testing has been done by Ng et al. (2014) to investigate the effects of consolidation on energy pile settlement. It is found that the settlement in lightly over-consolidated soil is more than the one in heavily over-consolidated soil when thermal cycles are applied to the energy pile because high over-consolidation ratio (OCR) soil tends to have less contraction.

Small-scale energy pile tests were performed by École des Ponts ParisTech (ENPC) France over the past few years (Kalantidou et al., 2012; Nguyen et al., 2017; Yavari et al., 2014a; Yavari et al., 2016b). Additional thermal settlement was discovered in the preliminary experiments (Kalantidou et al. 2012) a 600 mm aluminium pile is subjected to four different mechanical loads with two thermal cycles in a dry Fontainebleau sand, immediately after mechanical loading, and re-setting the experiment after finishing each test including soil compaction. They declared that the conventional factor of safety (FoS) is adequate for thermal loads too. Further analysis set-up was based on the preliminary experiments but with more accurate test procedures (Yavari et al. 2014a) First, the pile was loaded to failure to find the ultimate bearing capacity, then six thermo-mechanical tests were performed under 0 N, 100 N, 150 N, 200 N, 250 N and 300 N with temperature variations of ±5 °C. Higher accumulative

settlement was observed when higher loads were applied. Moreover, the long-term behaviour of the energy pile in sand was investigated with thirty thermal cycles applied instead of two thermal cycles. The pile continually settled after thirty cycles but tended to have decreasing increments, which means that more thermal cycles are required to reach pile stability in dry sand if the long-term settlement behaviour is considered. Simultaneously, thermal mechanical behaviour of energy piles in saturated clay in small-scale experiments was introduced (Yavari et al. 2016b). The result is in agreement with the dry sand test, and settlement is larger under higher axial loads. Under the same mechanical loads and similar temperature variation, energy pile settlement is smaller in saturated clay as compared to the case with dry sand. The latest published results present long-term thermo-mechanical behaviour of energy pile subjected in dry sand. Thirty thermal cycles applied at each test load, but stable settlement have not been reached (Nguyen et al. 2017).

2.1.4 Numerical simulations

Besides in-situ testing, Saggu and Chakraborty (2015) investigated the behaviour of a floating and end-bearing pile under several thermal cycles in loose and dense sand by finite element simulation. The results show that the first thermal cycle is important in settlement of the energy pile. Another research group concluded a similar result in the simulation study by Olgun et al. (2015), and pile head displacement and axial stress were investigated under three different equivalent climatic conditions for 30 years. The axial stress along the pile tended to increase even when the pile was progressively cooled after 30 annual thermal cycles. Thermal dilation differences between the pile and the soil during the thermal loading process could be the main reason for this effect.

The EPFL testing pile was also analysed numerically (Laloui et al., 2006). An axisymmetric geometric model was used with quadratic displacement, bi-linear pore water pressure and temperature elements in soil. The modelling pile adopted a radius of 0.5 m (0.44 m in the

experiment) and a length of 26 m, and the soil was sub-divided into five layers. The contact surface between the pile and the soil was considered as perfectly rough. The Drucker–Prager thermo-elastoplastic model was used for the soil and thermo-elastic behaviour for the pile. The simulation was in a good agreement compared to the results of the experimental data; the stress state of the pile was represented by FEM simulation.

Two centrifuge tests of geothermal energy piles were established by Ng et al. (2014) and its corresponding numerical simulation was performed by Loria et al. (2015), with a set of scaling factors to represent the actual pile behaviour. The centrifuge testing conclusion is reviewed in Section 2.1.3. Numerical simulation directly established a model for full-scale energy piles that corresponds to the centrifuge model. The numerical and experimental methods used in this study revealed that the higher the temperature variation, the higher the increase in vertical stress in the pile; and the higher the increase in thermal axial stress, the more stress transferred to the pile toe when the comparable temperature changes are 15 °C and 30 °C. In terms of pile axial load, the axial load distributions in the energy pile increase first, and then decrease with depth at the moment when the thermally- and mechanically-induced loads are working together. When mechanical load dominates the thermally-induced effect, the pile axial load decreases. A non-linear relationship was found in such cases. The simulation shows slight over-estimation for bearing capacity compared to the experimental results because a thin layer of standard finite elements with reduced mechanical properties was used at the soil-pile interaction surface. Further tests for higher temperature variation examined by simulation only (40 °C and 50 °C) show the null point is slightly below the geometric centre of the energy piles. In fact, the null point shifts upward when the pile experiences higher mechanical load, and downward when lower load is applied.

Fifty heating-cooling cycles in simulation are performed by Ng et al., (2016) to study the horizontal stress change of soil elements close to the pile. It shows that with thermal cycles

continuing, the horizontal stress along the pile depth progressively decreased. The settlement is irreversible due to the decrease of the shaft resistance. This is explained by the densification of soil below the pile toe and thus the decrease of the rate of the pile's settlement. Long-term thermo-mechanical behaviour of a floating pile in clay was studied by Vieira and Maranha (2016) under different mechanical loads and a temperature fluctuation for five years in the numerical study. Saturated and normally consolidated soil is considered in this study. It is concluded that the pile displacement is reversible during the thermal cycles if the pile works in a high factor of safety. In contrast, a lower factor of safety results in irreversible settlement and increases axial stresses with multiple cycles. Besides, Yavari et al. (2014b) introduced a simple method to simulate energy pile behaviour by ignoring thermal expansion of soil since they considered that most settlement that occurs in the pile mechanism is dominated by pile expansion. A commercial FEM software, Plaxis 2D, was used to repeat three in-situ energy pile mechanisms and it achieves relatively good agreement with the results obtained by in-situ tests in several experimental studies (Amatya et al., 2012; Bourne-Webb et al., 2009; Kalantidou et al., 2012; Laloui et al., 2003).

2.1.5 Pile design approaches

Probabilistic analysis of energy piles was reported by Xiao et al. (2016). Four different uncertain parameters were used in this study: internal friction angle (ϕ'), Menard pressure meter modulus (EM), spring constant (Kh) and mechanical load (P). Through sensitivity analysis from ultimate limited state and serviceability limited state assessment, they determined friction angle and Menard pressure meter modulus are the two most sensitive parameters, and then performed a probability study based on a hypothetical energy pile of 20 m in length with a diameter of 0.6 m. Probability calculations are dominated by the factor of safety and limiting settlement. The thermal loading may cause additional uncertainty to the structure rather than the factor of safety only, so further consideration for probability is necessary when designing

geothermal energy piles. Mimouni and Laloui (2014) declared that overdesigning a geothermal energy pile is insufficient in terms of serviceability according to their factor of safety (FoS) study and increases the construction costs.

2.2 Thermal performance

Thermal performance analysis determines utilisation of this application into commercial construction. Many researchers conducted thermal performance studies of geothermal energy piles (Carotenuto et al., 2017; Gao et al., 2008a; Ghasemi-Fare & Basu, 2013; Miyara et al., 2011; Murphy et al., 2015; You et al., 2014). The heat exchange function in geothermal energy piles is usually implemented by constructing a water circulation pipe inside the reinforcement cage. The majority of studies focus on configuration of this water circulation pipe to ensure thermal exchange rates are sufficient to meet thermal performance requirements. The thermal behaviour of energy foundations is reviewed here to give us general ideas for HVAC practice.

2.2.1 In-situ thermal testing for a single pile

You et al. (2014) established several energy piles on a construction site to study thermal performance. Seven cement fly ash gravel (CFG) piles, 420 mm in diameter and 18 m in length, were constructed in a line with 2 m spacing between the piles. A W-shaped water pipe was used inside the pile. Four tests were performed for a single pile test: control heat flux, control temperature, control flow rate and control operating time. They found that even though larger heating power resulted in larger inlet/outlet temperature differences, the thermal conductivity of the soil was decreasing because heating reduced the water content of the soil. The linear response is found between the inlet temperature increase and the heat exchange rate. It is interesting that a non-linear relationship was discovered for the flow rate influence of heat exchange rate, which can be explained by insufficient thermal exchange if the flow rate is high. The heat exchange rate under continuous operation is smaller than the intermittent operation.

They also studied thermal performance of grouped piles which will be discussed in Section 2.2.3.

Similar behaviour was observed by Murphy et al. (2015), as a relatively rapid rise in temperature was observed in the first 25 h. Because of the ambient temperature effect, the deeper part of the surrounding soil has a more stable temperature than the upper part near the surface, while the temperature in the upper part fluctuates in hot weather. In terms of thermal exchange rate, the values of heat exchange rate range from 24.4 to 108.5 W/m in the 15.2 m length of the pile, which agrees with the values obtained by You et al. (2014). Both studies reported a soil thermal conductivity drop while the energy pile was in operation. Murphy et al. (2015) further investigated this phenomenon and found that the temperature gradient between the foundation and the adjacent boreholes became steadier, which approaches to a constant thermal conductivity value after 400 hours.

A water pipe configuration experiment was conducted by Miyara et al. (2011). Three different pipe types, U-tube, double-tube and multi-tube, were considered in this study with a 20 m length of steel screw pile. Three different flow rates, 2 L/min, 4 L/min and 8 L/min were also compared with the pipe shape. The double-tube in the experiment shows the highest heat exchange rate since a larger quantity of water storage provided optimum thermal storage with the surrounding soil, which gives a larger heat exchange rate. In the flow rate study. However, an increasing heat exchange rate was observed with flow rate increases in all cases, unlike the non-linear response found by You et al. (2014), which means that the flow rates chosen are all within sufficient heat exchange range in this study.

2.2.2 Numerical simulations

Similar to the energy pile mechanism study, numerical simulation gives us more detailed information for thermal performance studies. A finite difference code developed by Ghasemi-

Fare and Basu (2013) aims to investigate the thermal performance of energy piles based on U-tube pipe line configuration in an axial symmetric model. Through the code, they concluded that 11 times the pile radius, 11 r_p, is the upper bond of thermal influence zone for single piles and the zone is independent from temperature differences and water circulation velocity, but temperature gradient increases within the soil body with water circulation velocity increases. The heat flux decreases with the pile length and reduced almost 30% within the first day of operation. In terms of parameter sensitivity, energy output is most influenced by temperature difference of circulation fluid, soil thermal conductivity, and radius of heat carrier tube. This agrees with the experiment of Miyara et al. (2011), where the double tube has the largest surface area of circulation tube, so it has the largest thermal exchange rate. The smallest impact factor for energy output is thermal conductivity of the structural pile, fluid flow rate and radius of pile.

A 3-D finite element model aimed at studying parametric and pipe configuration influence was reported by Carotenuto et al. (2017). A single U-tube, double U-tube, triple U-tube and spiral coil shape with variance of pitch distance were considered in this study by using COMSOL Multiphysics. Unlike previous literature (Ghasemi-Fare & Basu, 2013), the finite element simulation shows that thermal conductivity of structural piles and fluid flow rates play an important role in heat transfer. But they both agree that the radius of a pile does not significantly influence heat exchange rate. A spiral coil shape pipe configuration, in this study, provided the largest temperature difference output and narrow pitch distance, from 0.7 m to 0.25 m, producing 68% increase of heat transfer performance.

The heat exchange rate between W-shaped heat exchangers and 3U-shaped heat exchangers was examined by Park et al. (2013). They implemented two subroutines into commercial finite element software ABAQUS to simulate the water circulation process inside the energy pile. A 10 m (X) × 10 m (Y) × 16 m (Z) soil body was modelled with a 0.4 m diameter, 13.25 m depth

(W-shape) and 13.75 m depth (3U-shape) energy pile. The pile dimension was the same as in-situ experiments that had been performed. Both intermittent and continuous operation were studied. The simulation shows that heat exchange in the 3U configuration produced a higher temperature rise, which is slightly larger than the W-shaped pipe configuration. Increasing the pipe length results in an increase of heat exchange rate in the intermittent operation condition, but the continuous operation is not affected. The intermittent operation seems to be more suitable than the continuous operation in application because of the high exchange rate and ground temperature recovery, but it loses thermal energy and has time limitations in operation. Other researchers confirm these findings (Faizal et al., 2016; Yang et al., 2016).

2.2.3 Group piles

Bezyan et al., (2015) established a model with energy pile groups. Serial and parallel connections with just one main water pump in the heat pump system was located at the beginning of the pipeline. Nine piles in serial connection and 15 piles in parallel connection are studied here. The results show that the outlet temperature of water decreased roughly 16.7 °C, which is approximately the mean ground temperature of the nine piles in serial connection, but the temperature drop in the parallel connection with 10 piles is 13.2 °C, which is less than the serial connection — not a remarkable temperature drop as in the 11–15 piles which is 1.2 °C. Dupray et al. (2014) studied temperature losses in group energy piles by 2D simulation and the change of soil temperature towards an equilibrium after years of operation. Working at higher temperatures does not significantly increase thermal losses. Namely, thermal efficiency remains based on the difference between the annual mean storage temperature and the natural ground temperature.

2.2.4 Analytical solutions for borehole heat exchangers

Analytical solutions for borehole heat exchangers provide an idealised case to estimate temperature change within a soil body. The summarised analytical solutions can be found in

Ghasemi-Fare and Basu (2013). Overall, there are six heat source models describing geothermal heat exchangers, namely: infinite line source model, finite line source model, infinite hollow cylinder model, infinite solid cylinder model, finite solid cylinder, and spiral line model (Carslaw & Jaeger, 1959; Ingersoll, 1954; Li & Lai, 2012; Man et al., 2010; Zeng et al., 2002). Three of these models, the infinite line source model, the finite line source model and the infinite solid cylinder model, have been selected to describe below.

1. Infinite line source model (Ingersoll, 1954) describes an infinite long line heating source within solids, and the spatial and temporal temperature increment is given by the following equation:

$$\Delta T(r,t) = -\frac{\dot{q}_l}{4\pi k} E_i\left(\frac{-r^2}{4\alpha t}\right). \qquad 2.1$$

The other analytical solutions for heating conduction related to borehole heat exchangers is developed based on this fundamental solution.

2. Finite line source model by Zeng et al., (2002):

$$\Delta T(r,z,t) = \frac{\dot{q}_l}{4\pi k}\int_0^L \left\{ \frac{erfc\left(\frac{\sqrt{r^2+\left(z-z'\right)^2}}{2\sqrt{\alpha t}}\right)}{\sqrt{r^2+(z-z')^2}} - \frac{erfc\left(\frac{\sqrt{r^2+\left(z+z'\right)^2}}{2\sqrt{\alpha t}}\right)}{\sqrt{r^2+\left(z+z'\right)^2}} \right\} dz' . \qquad 2.2$$

3. Infinite solid cylinder model as introduced by Man et al. (2010):

$$\Delta T(r,t) = \frac{\dot{q}_l}{4\pi k}\int_0^\pi \frac{1}{\pi} Ei\left(-\frac{r^2+r_0^2-2rr_0\cos\varphi}{4\alpha t}\right) d\varphi . \qquad 2.3$$

Note, for all equations above, where:

$$E_i(x) = \int_{-\infty}^{x} \frac{e^u}{u} du , \qquad 2.4$$

and *erfc* stands for error function. Here k is thermal conductivity (W/mK); L is length of the heat source (m); r_0 is cylinder radius (m); r, z, and φ are the cylindrical coordinate system; $\dot{q}_l$ is the heat flux per unit length (W/m); t is time; T is temperature; α is thermal diffusivity (m^2/s); and ρ is mass density (kg/m^3).

The analytical solution gave us the best prediction of temperature distribution to estimate the thermal response within a soil body in a certain time; however, there are limitations, as follows: (1) Homogeneous soil conditions must exist, and (2) multiple heating sources in a close distance cannot be achieved by superimposing temperature responses. Therefore, the finite element simulation is introduced and modelled for the study of thermal performance of multiple piles.

2.3 Summary

Previous studies identified recent research progress and provided a general picture of the application of geothermal energy piles. To achieve the goal of this thesis, further investigation for long-term thermo-mechanical behaviour of energy piles is required although some literature reported short-term mechanism of energy piles, it is still unclear in terms of its behaviour under thermal cyclic loading conditions. Furthermore, energy losses in pile grouping arrangement requires more investigation. Commercial finite element software, ABAQUS, is selected to perform numerical studies since it satisfies the requirement of modelling and loading conditions based on existing literature and experiments. This provided motivation to study on this topic.

Chapter 3. Methodology

In this Chapter, we focus on thermo-mechanical analysis of energy piles and thermal performance analysis of pile group under long-term thermal cycles. A physical model to investigate the energy pile response when subjected to thermal cycles was established and instrumented at the Lab Navier-Géotechnique, École des Ponts ParisTech (ENPC), France, while The University of Sydney performed a parallel simulation study based on the finite element method. This study is based on a series of previous researches conducted at ENPC, while the majority of studies are focused on physical experiments (Kalantidou et al., 2012; Nguyen et al., 2017; Yavari et al., 2014a; Yavari et al., 2014b; Yavari et al., 2016b). Moreover, according to the literature review in Chapter 2, most researches on thermal performance studies (Carotenuto et al., 2017; Dai et al., 2016; Franco et al., 2016; Gao et al., 2008b; Signorelli et al., 2007) are based on single pile thermal performance. Pile grouping thermal performance is unclear or less reported with respect to HVAC engineering practice.

3.1 Thermo-mechanical analysis of energy piles

The physical pile model was established initially for pile in dry sand referring to Yavari et al. (2016b), and now extended for saturated clay see Figure 3.1. A bottom sealed aluminium tube with internal and external diameters of 18 mm and 20 mm, respectively, was made to represent the energy pile in the experiment with a length 800 mm. The external surface of the pile was sand-coated in order to reproduce the roughness of a full-scale bored pile under real construction conditions. Also, 600 mm of the full 800 mm length was embedded into saturated clay.

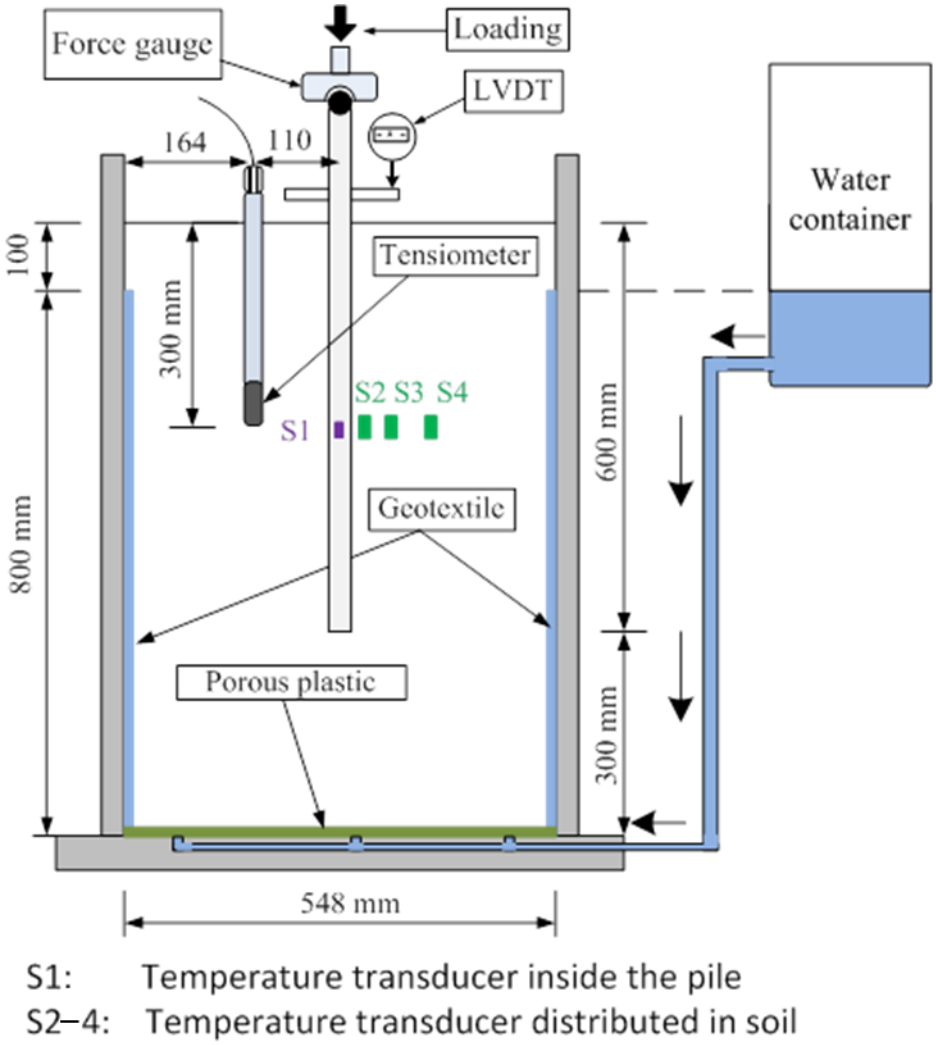

Figure 3.1 Experimental setup of a single physical pile model in saturated clay.

A U-shaped water circulation tube was assembled inside the aluminium pile. A temperature sensor was placed inside the pile at a depth of 300 mm to monitor the temperature during the experiments. The axial load control is at the pile head, by deadweight only (more details can be found in Yavari et al. (2014a) on a similar setup) and measured by a force sensor. The displacement at the pile head is measured by a displacement sensor located close to the soil's top surface. Three sensors are installed at 300 mm depth and 20, 40, 80 mm from the pile axis to record the temperature distribution inside the soil body. Speswhite Kaolin clay was used in this study. Compaction was performed to ensure homogeneity for soil quality. The soil mass after compaction was determined as a dry density of 1.45 mg/m^3 (degree of saturation 95% and void ratio 0.79).

Soil samples were cored in 20 mm diameters from the compacted soil mass for the determination of dry density and water content to control the quality of the compaction procedure. As expected, the dry density and the water content are relatively uniform with depth and close to the designed values (Figure 3.2). A porous plastic plate and geotextile layer were installed at the bottom and lateral surface to speed up the saturation process. The water level in the water container was kept 100 mm below the soil surface to avoid water overflow on the soil surface. The results shown in Figure 3.3 demonstrate the progress of soil suction as it approaches zero after 18 days. The apparatus was kept for a total of 45 days to ensure the soil achieved full saturation. The temperature of the soil and piles was kept at room temperature, 20 °C, for one week. More details about temperature and quality control can be found in (Nguyen et al. 2018).

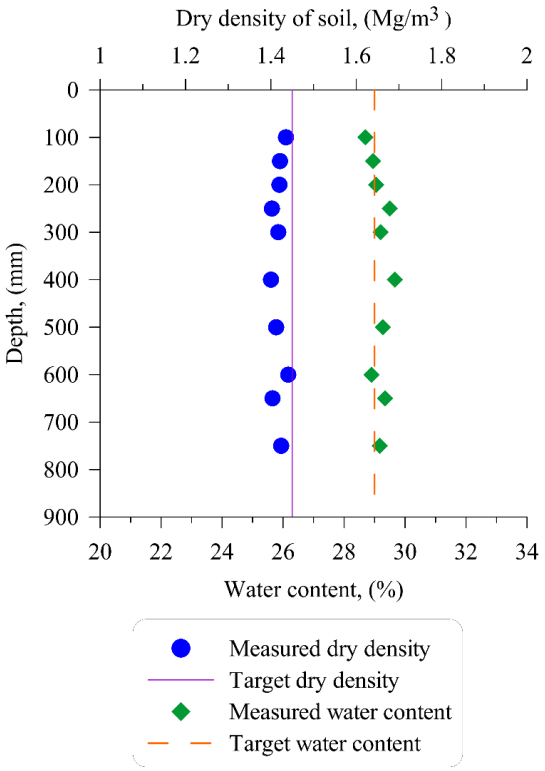

Figure 3.2 Dry density and water content of compacted soil

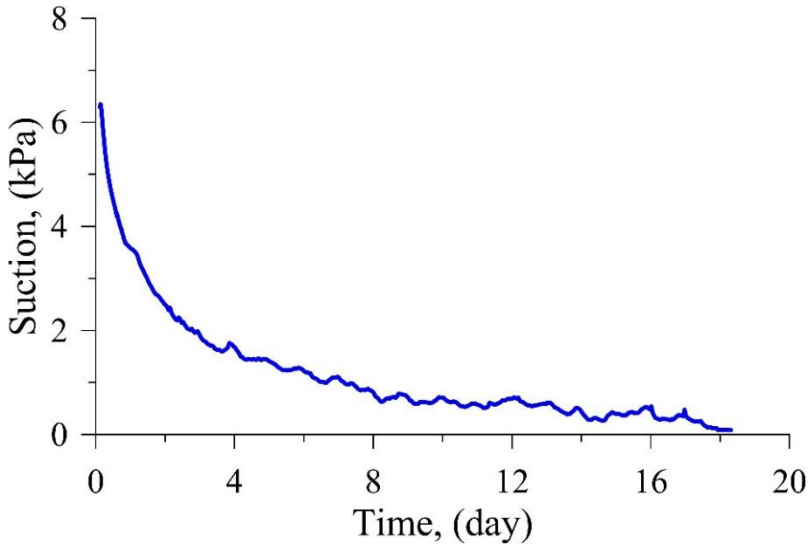

Figure 3.3 Evolution of soil suction during the saturation process (measured by tensiometer)

After the experiment's quality control process, the pile was loaded to failure for estimating its ultimate load bearing capacity (test A1). The pile head was mechanically loaded with increments of 50 N in a series of steps, and maintained for one hour in each step; the procedure is compliant with French Standards (Afnor 1999).

In test A1, 500 N was loaded on the pile head, corresponding to the pile's ultimate bearing capacity. After that, the pile head load was removed. Followed by test A2, no load was applied to the pile head during this test and 30 thermal cycles were performed straight away. Then, the pile head was loaded to 20% of the pile's capacity (100 N) prior to the 30 thermal cycles (test A3). At the end of these cycles, the pile head load was removed and left for the pile to naturally heave into steady position. Further, 40% of the pile's ultimate load was applied and then 30 thermal cycles were performed under test A4. Test A5 was conducted with a similar procedure, corresponding to 60% of the pile's ultimate capacity. A similar procedure can be found by Yavari et al. (2016b), but only one thermal cycle was applied after each mechanical load test. The aim of the purely mechanical test (A1) is to identify the pile's ultimate capacity. The

ultimate bearing capacity load test would not influence thermo-mechanical behaviour of the pile during the subsequent tests (Yavari et al., 2016b).

The pile temperature changes vary from 21 °C to 19 °C, which is ±1 °C around room temperature. This temperature variation of the energy piles in this case is much smaller than the range is some other studies, sometimes reaching up to ±20 °C (Di Donna & Laloui, 2015; Olgun et al., 2015). In fact, the study in this small-scale model has the dimension of a 20 mm pile diameter, which is 20 times smaller than a full-scale pile of 0.4 m in diameter, and 12 m length in the full-scale model. Therefore, the strain related to the mechanical behaviour is 20 times smaller than that at the full-scale load, especially in terms of thermal expansion (Laloui et al., 2006; Ng et al., 2014). In this study, the temperature change reduced 20 times to ±1 °C based on this discussion in order to comply with the thermal strain rate in the full-scale model. Each thermal cycle operated for 24 hours, which includes a 4-hour heating period, followed by a 4-hour cooling period, and the remaining time is occupied by a reheating period that allows the energy pile to return to initial room temperature.

The finite element simulation is carefully modelled by considering the preparation and loading details from this experimental procedure in order to get reliable simulation outcomes. Details of the simulation procedure and its results are reported in Chapter 4. The results from the experiment and simulation are shown in Figure 3.4. The load-settlement response is similar to Yavari et al. (2016b) as it has a similar experimental set-up, and the results ensure repeatability of the experimental procedure applied in the current experiment.

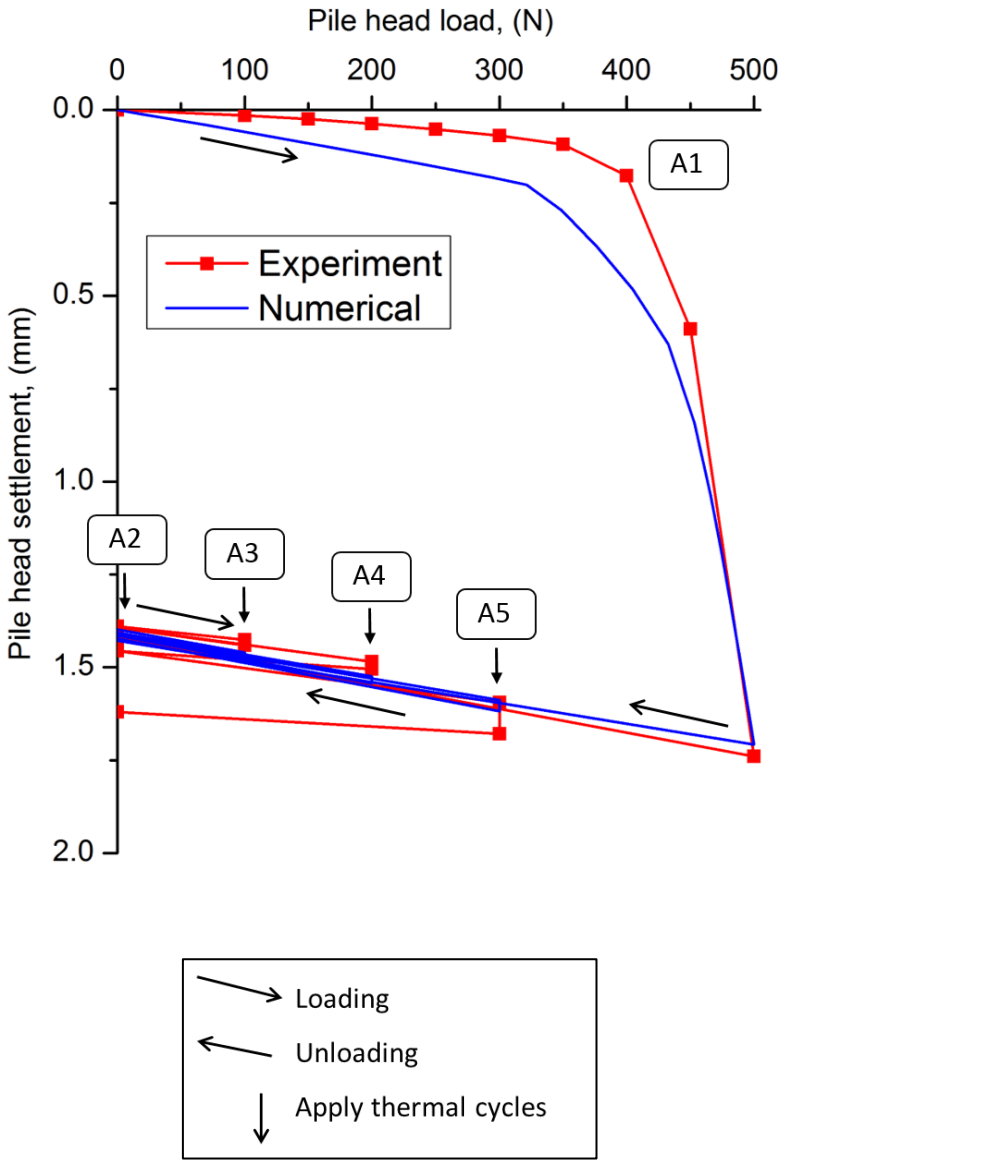

Figure 3.4 Pile head load displacement curve: A1 is a purely mechanical test; A2, A3, A4 and A5 are thermo-mechanical tests

3.2 Thermal performance analysis of pile groups

In this study, we assume that the total energy extraction of geothermal energy piles from natural ground temperature can be measured by total heat flux on the surrounding pile core. As such, the finite element model is simplified and compared with cases of fully coupled and explicit simulations with circulated fluids. Firstly, the equivalent heating zone is introduced here and has been studied in a single pile model. This method is benefitted by a simplified simulation technique and the focus here is to compare the thermal performance of a variety of pipe configurations. Saving computational resources allows larger-scale and pile groups to be modelled effectively. Although the drawback is obvious that at least one in-situ test is needed, finding an accurate equivalent heat zone and fluid outlet temperature cannot be measured. This equivalent method is capable of investigating the energy extraction behaviour of geothermal energy pile groups. Figure 3.6 (a) shows the dimensions of equivalent zone and single pile model, 10×10×16 m as shown in Park et al. (2013). The energy pile is divided into three parts: pre-cast high strength concrete (PHC) outer core, grout concrete inside circular hollow PHC cylinder, and equivalent heating zone. The diameter of the equivalent heating zone can be tuned to fit any type of circulation pipe configuration. In this case, W-shaped and 3U-shaped configurations are modelled by matching the heat exchange rate during continuous operation. Figure 3.5 is shown here for W-shaped pipe configuration results for a ninety-day continuous operational mode, compared with the fully coupled and explicit simulation by Park et al. (2013). It is noted that the heat extraction surface is between the PHC and the grout (where the water circulation pipe is installed), 4.75 m below the top to avoid ambient temperature effects. It is obvious that the method is in a good agreement after tuning the equivalent diameter. Further explanation is given in Chapter 5. Table 3.1 presents the dimensions of different pile diameter divisions with the determined equivalent heating zone dimensions.

Table 3.1 Simulation dimensions

Configuration/dimensions	W-shaped	3U-shaped
D_{PHC} (m)	0.4	0.4
D_{grout} (m)	0.22	0.24
$D_{heating}$ (m)	0.140*	0.168*
h (m)	13.25	13.75

* Equivalent value determined by simulation results.

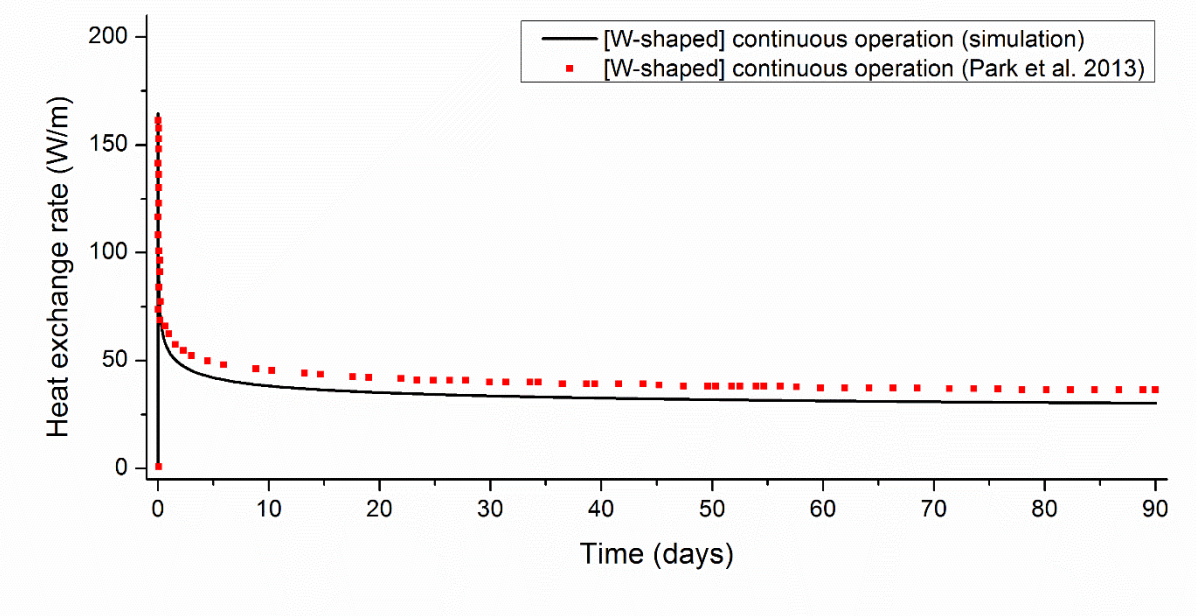

Figure 3.5 Heat exchange rate of W-shaped configuration for 90 days

After the single pile, two groups of pile models have been established based on 3U-shaped configurations, since 3U-shaped water pipes have a relatively large thermal exchange rate compared with the W-shaped pipe configuration, as found by Carotenuto et al. (2017) and Park et al. (2013). Two × nine pile simulation models with centre-to-centre spacings of 1 m and 2 m are used. According to Australian construction practice, the minimum centre-to-centre spacings in pile construction is 2.5D (where D is the pile diameter) if the end-bearing pile is subject to bedrock. In this case, the minimum spacing is 1 m. Further, the 2 m centre-to-centre spacing

case is also modelled to study distance effect, see Figure 3.6 (b) and (c). The nine piles are heating simultaneously to 30°C as inlet fluid temperature. One complete heating cycles includes 8 hours heating and 112 hours off-mode to allow ground temperature to have sufficient time to recover, which ends up being roughly five days, as reported in Park et al. (2013). Twenty cycles (100 days) of simulations are performed by applying multiple thermal cycles to ensure thermal exchange rates reach relatively static state conditions. Pile 1, Pile 2 and Pile 5 are selected as typical pile locations in this study since it represents a corner pile, edge pile and centre pile, respectively. The aim of this study is to investigate different adjacent pile positions and distance effects of thermal exchange rates. By comparing the results from different pile distances, a clearer picture for thermal performance of geothermal energy pile groups will be presented.

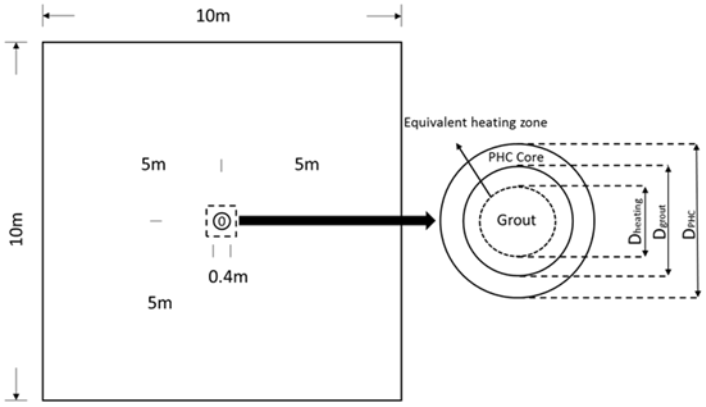

(a) Plane view of single pile dimension and pile inner core defined dimensions, with the left insert showing the proposed equivalent heating zone model

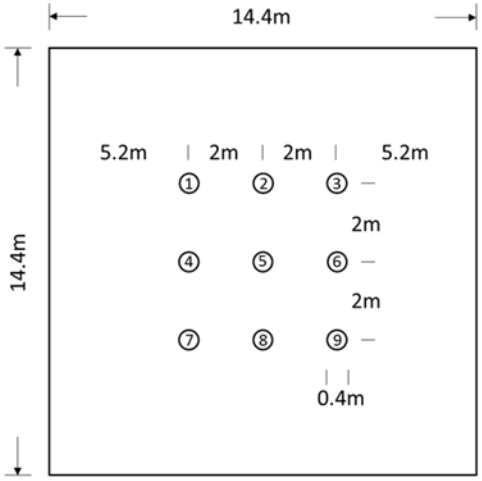

(b) Plane view of group pile centre-to-centre spacings at 2 m

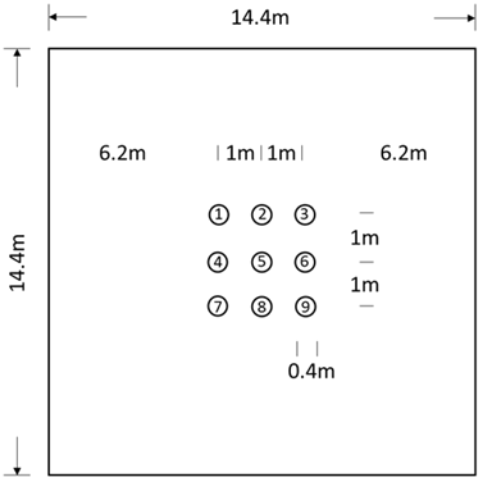

(c) Plane view of group pile centre-to-centre spacings at 1 m

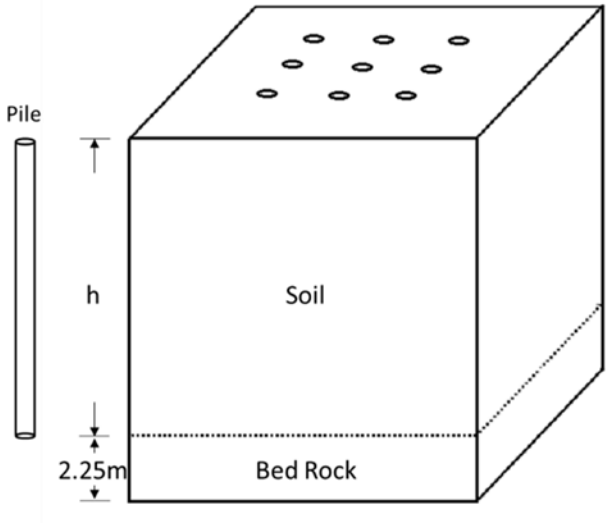

(d) 3D view including height

Figure 3.6 Dimensions of energy pile(s)

After simultaneous heating of the nine piles, a cross-pile heating strategy is followed for both cases (the 1 m spacing and 2 m spacing scenarios). Pile numbers 2, 4, 6 and 8 are Group 1; and the rest of the piles, 1, 3, 5, 7 and 9 are Group 2. Heating cycles alternate from Group 1 to Group 2 with the same duration as the simultaneous heat case. The duration for each cycle has been shortened to 2.5 days compared with the fully operational mode. Namely, the first thermal cycle includes 8 hours of heating, followed by 52 hours off-heating to let the pile temperature naturally drop in group 1; and keep repeating this process at the second thermal cycle in group 2. Thermal cycles are repeated 20 times (20 thermal cycles and 50 days). This is to ensure that the same amount of heat is injected to the system within 5 days as 9 piles in simultaneous heating cycles. Against the 2.5-day cycle, 5-day cycles are also modelled for comparison and discussion in terms of soil heat recovery. Five-day cycles are also repeated 20 times, which is 100 days in total time for the simulation. The average power will be studied and plotted to represent an entire heating cycle strategy. The strategy allows us to investigate the optimum arrangement for geothermal pile performance. Table 3.2 summarised all scenarios in this study.

Table 3.2 Case study scenarios.

Operation mode	Pile centre-to-centre spacing (m)	Period(s)
All piles (full operation)	1	8 hours heating,112 hours off
All piles (full operation)	2	8 hours heating,112 hours off
Alternate heating (Pile group 1-> Pile group 2)	1	Pile group1: 8 hours heating, 52 hours off Then Pile group2: 8 hours heating, 52 hours off
Alternate heating (Pile group 1-> Pile group 2)	2	Pile group1: 8 hours heating, 52 hours off Then Pile group2: 8 hours heating, 52 hours off
Alternate heating (Pile group 1-> Pile group 2)	1	Pile group1: 8 hours heating,112 hours off Then Pile group2: 8 hours heating,112 hours off
Alternate heating (Pile group 1-> Pile group 2)	2	Pile group1: 8 hours heating,112 hours off Then Pile group2: 8 hours heating,112 hours off

*Pile group 1 are pile#: 2, 4, 6, 8 and Pile group 2 are pile#: 1, 3, 5, 7, 9 in Figure 3.6.

Chapter 4. Long-term Thermo-mechanical Behaviour

Energy pile foundations are subjected to heating-cooling cycles year after year, corresponding to seasonal temperature fluctuations. These annual thermal cycles change the soil/pile interaction behaviour from a thermo-mechanical point of view. Despite some studies focusing on the thermo-mechanical behaviour of energy piles in short periods or cycles, few researches have been found that investigate the long-term behaviour of energy pile settlement. In these studies, numerical methods are usually used, and experimental methods are mainly based on physical modelling.

In this chapter, the work is in conjunction with the work of the Lab Navier-Géotechnique, École des Ponts ParisTech (ENPC), France. First, a small-scale pile model installed in saturated clay was examined and tested at ENPC. Thirty thermal cycles were applied whilst the pile head load was maintained constant at 0%, 20%, 40% and 60% of pile bearing capacity. Second, the finite element method was used for comparison to numerically simulate the experiments at The University of Sydney. The results of the two methods are analysed simultaneously in order to have better identification for the main mechanisms that dominate the thermo-mechanical behaviour of energy pile thermal cyclic loading conditions. The work consists in integrating results of a small-scale pile model (physical modelling) with those obtained by numerical modelling (finite element numerical model), with a specific focus on the long-term mechanical effect on energy geostructures (energy piles, in the present case) under thermal cycles.

4.1 Numerical modelling

4.1.1 Axisymmetric finite element model

Finite element analysis was performed using the commercial FEA software, ABAQUS V6.16. To model the physical experiment, a two-dimensional axisymmetric model was established (as

shown in Figure 4.1) and fully coupled four-node temperature-pore pressure-displacement element (CAX4PT) and four-node bilinear displacement-temperature elements (CAX4T) were used for the regions of the soil and pile, respectively. Soil is assumed to be fully saturated throughout the loading cycles, and the top 100 mm capillary zone in the physical model is ignored. Pore pressure at the top surface of the soil is opened to air, but no heat flow escapes from the top surface. A circular hollow section aluminium pile is modelled by solid piles with the equivalent mass density. Soil is modelled by the modified Cam-clay model and the pile is described by a linear-elasticity model. For contact properties, the friction coefficient at the soil-pile interface is assumed to be tan ϕ, where ϕ is the soil friction angle. Note that a relatively large thermal conductance is chosen at the pile-soil interface to reduce the interfacial thermal contact resistance. Lateral pressure coefficient is assumed based on the Meyerhof correlation, $K_0 = (1 - \sin\phi)\mathrm{OCR}^{0.5}$, by taking the pressure at 2/3 depth of the pile for averaging pressure along the pile to estimate K_0, and OCR is approximately 160. The calculation of OCR is based on the ratio of the historical maximum pressure and the current experienced pressure. The former is calculated based on the Cam-clay model parameters from Lv et al. (2017) for NCL, *i.e.* 560 kPa with the experimentally measured void ratio of 0.79. As a result, K_0=8 is adopted for the numerical simulation and it is within a reasonable range since preparation of the physical model involves a pre-compaction process. All parameters in simulation are summarised in Table 4.1 and Table 4.2, and the constitutive parameters of soil can be referred to in Lv et al. (2017). The initial temperature for the entire numerical model is assumed to be 20 °C as the case for the physical model. The bottom and side boundaries are set as the constant temperature at 20°C. Deformation of soil is fully fixed at the bottom and is only horizontally fixed at the side, while the top surface is free to deform. Initial geostatic displacement tolerance was set at 0.6 mm, while calculated vertical displacement of soil after geostatic balance is

93.28×10^{-6} mm; the calculated tolerance is much less than the displacement sensor (LVDT, with accuracy ±0.001 mm). Finite sliding formulation is used at the soil-pile interface.

Temperature variation with time in the physical experiment is deemed to be an input parameter to investigate settlement occurring under the cyclic thermal loading condition. To simplify the model, the entire pile is going to experience temperature variation uniformly instead of the water circulation process in the experiment. Thirty heating and cooling cycles are applied in every thermal loading stage after the given mechanical load. One complete thermal cycle includes four different thermal phases: initial, heating, cooling, and reheating, which will induce settlement fluctuation. The modelling details can be found in Nanwangzi and Yixiang (2017).

Table 4.1 Parameters of pile and soil in numerical modelling

Parameters	**Pile (CHS aluminium)**	**Clay (Speswhite Kaolin Clay)**
Constitutive model	Linear-elastic	Modified Cam-clay
Dry density (Mg/m^3)	1.32	1.45
Volumetric weight at saturated state (kN/m^3)	N/A	18.53
Young's modulus E (kPa)	1.3E7	N/A
Poisson's ratio v*	0.33	0.25
Slope of critical state line M*	N/A	0.98
Slope of virgin consolidation line λ*	N/A	0.14
Slope of swelling line κ*	N/A	0.012
Initial void ratio e_0*	N/A	1.6
Void ratio after compaction e_1	N/A	0.79
Friction angle ϕ*	N/A	25°

Permeability k (m/s)*	N/A	1E-8
Thermal expansion (/°C)	2.3E-5	1E-6
Thermal conductivity (W/m°C)	237	1.5
Specific heat capacity (J/kg°C)	9E2	1.269E3

* Soil properties are adopted from Lv et al. (2017)

Table 4.2 Other relevant parameters in numerical modelling

Volumetric weight of water (kN/m^3)	9.81
Friction coefficient tan ϕ	0.47
Interfacial thermal conductance (W/°C*m^2)	500
Lateral earth coefficient, K_0	8

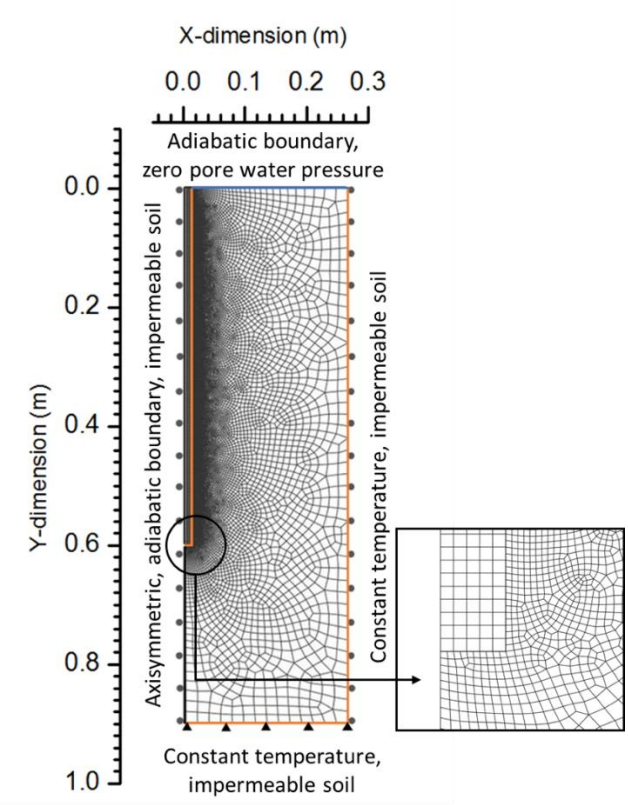

Figure 4.1 Geometry and boundary conditions of the numerical model

4.1.2 Mesh sensitivity study

Five different mesh convergence analyses were performed to study mesh dependency of the numerical model. For the pile, uniform 1 mm, 2 mm and 3 mm seed sizes were applied in the pile region with an unchanged 1 mm mesh size on the soil side of the soil-pile interface in order to find the appropriate pile mesh size. It is found that the 2 mm pile mesh size was sufficient. Then, mesh sizes of 1 mm, 1.5 mm and 2 mm were applied to the soil side of the soil-pile interface region, which enables a total of five different types of mesh size combinations. At the far end, bottom and side of the soil, the mesh seed size was set to a fixed 20 mm value for all simulations. Here, only the purely mechanical loading condition, A1, was considered for this mesh convergence study, which was similar to Wehnert and Vermeer (2004) work. In Figure 4.2, load and settlement curves for different mesh size combinations are given. As a result, (Pile 2 mm, Soil 1 mm) the mesh is selected by considering both accuracy and computational time.

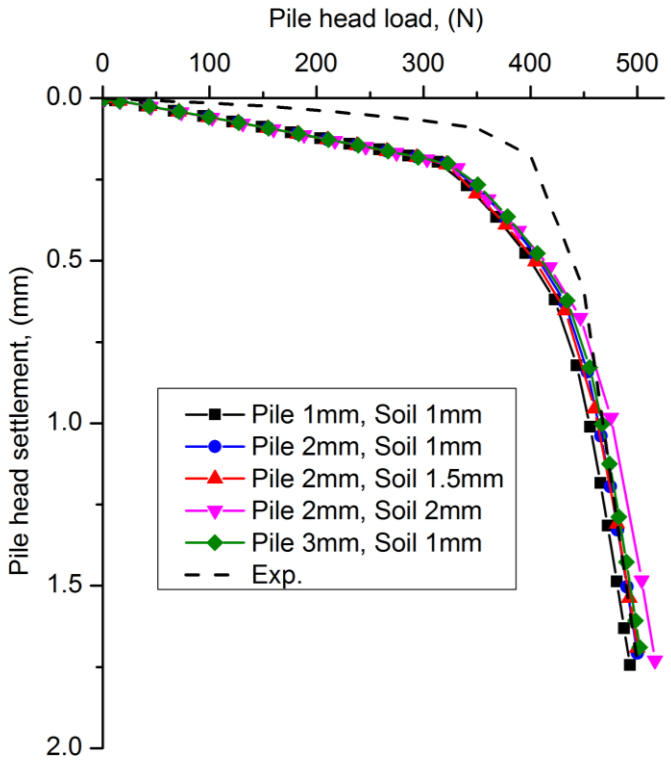

Figure 4.2 Mesh dependency results (A1)

4.2 Results

4.2.1 Mechanical behaviour of pile

The experiment results of test A1 are shown in Figure 3.4 in Chapter 3. This load-settlement curve is based on the settlement value at the end of each load step. After loading to 500 N, the pile is unloaded and the irreversible settlement of the pile head is about 1.42 mm. The relationship between the axial load and the pile head settlement during the loading is almost linear when the axial load is smaller than 350 N. For axial loads higher than this value, pile head settlement increases significantly with an increase in axial load. The numerical result gives similar behaviour of the pile by using the parameters of the pile and the soil as shown in Tables 4.1 and 4.2. Analysis of the plastic points show that during the loading path, when the axial load is lower than 350 N, only few plastic points can be observed at the pile toe. Interfacial friction is approaching maximum shear stress and loading above this value induces development of plastic zones — this phenomenon can be observed by the quick increase of pile head settlement.

4.2.2 Thermo-mechanical behaviour of pile

In this section, the results of the tests from A2 to A5 are presented. Figure 4.3 shows the temperature distribution corresponding to four phases of one thermal cycle: initial, heating, cooling, and reheating. These results confirm that the heat transfer between the pile and the surrounding soil is mainly radial along the pile. The temperature measured at the 300 mm depth (in the middle of the pile) should be then representative to study the heat transfer in this study.

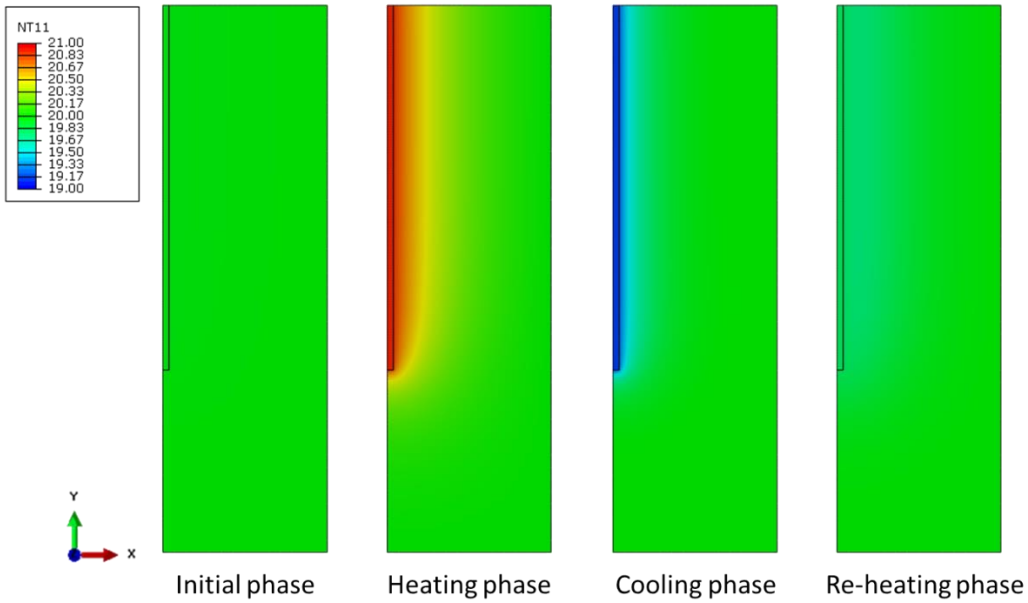

Figure 4.3 Temperature distribution during one thermal cycle obtained from numerical modelling

Figure 4.4 presents the temperatures measured at different locations along the 300 mm depth during one thermal cycle. These measurements show that the soil temperature increases when the pile is heated and decreases when the pile is cooled. The effect of pile heating/cooling is more significant for sensors located closer to the pile. The numerical results obtained in the soil are in good agreement with the experimental ones. This agreement confirms that the thermal parameters and the heat transfer mechanisms (heat conduction) used in the numerical model are appropriate. Note that the thermal parameters have been determined separately in the laboratory by a thermal probe.

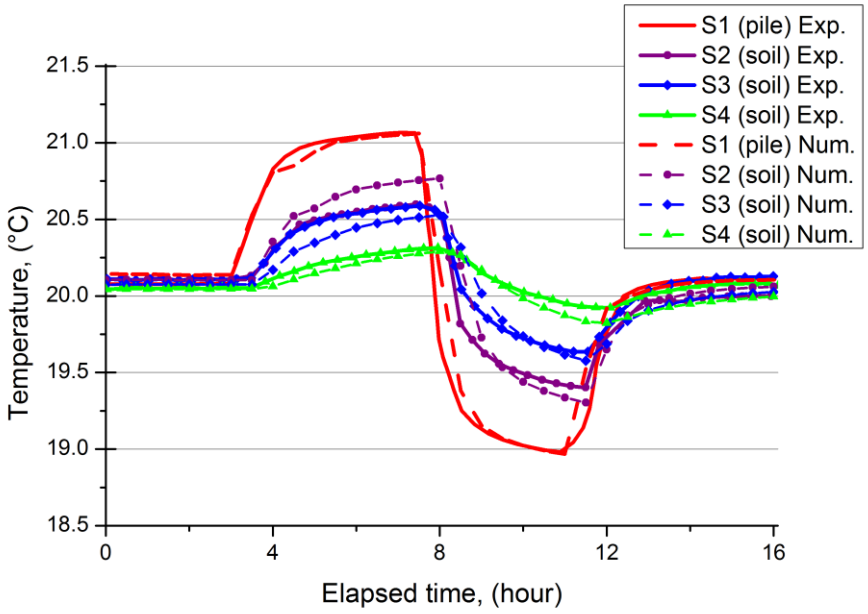

Figure 4.4 Temperature of pile and surrounding soil during one thermal cycle (Num. = Numerical results, Exp. = Experimental results)

Figure 4.5 shows the results of temperature and displacement of the pile over the 30 thermal cycles under different loads. It can be seen that the target temperature (20 °C – 21 °C – 19 °C – 20 °C) in each thermal cycle could not be strictly respected during the first test (A2). This is related to the variation of temperature in the room. For this reason, in the subsequent tests (A3, A4, A5), the thermal isolation of the tube connecting the cryostat and the pile was improved, allowing the influence of room temperature on the pile temperature to be reduced significantly. In Figure 4.5, the pile head settlement of each test is set to zero at the beginning of the thermal cycles. The results generally show pile head heave during heating, and settlement during cooling. However, the relation between the pile head displacement and the pile temperature is not strictly reversible. Note that the temperature was controlled manually and for some cycles corresponding to weekend periods, the active heating phase took longer than two days. Nevertheless, it seems that these longer phases do not significantly influence the results.

In the numerical model, the pile temperature measured in the experiment is imposed on the whole pile to simulate the thermal cycles under constant pile head load. The pile head settlement obtained by the simulation is also shown in Figure 4.5. The numerical results show equally a pile head heave during heating and settlement during cooling. More details on pile head displacement during each thermal cycle and the irreversible pile head displacement are shown in Figure 4.6 and Figure 4.7.

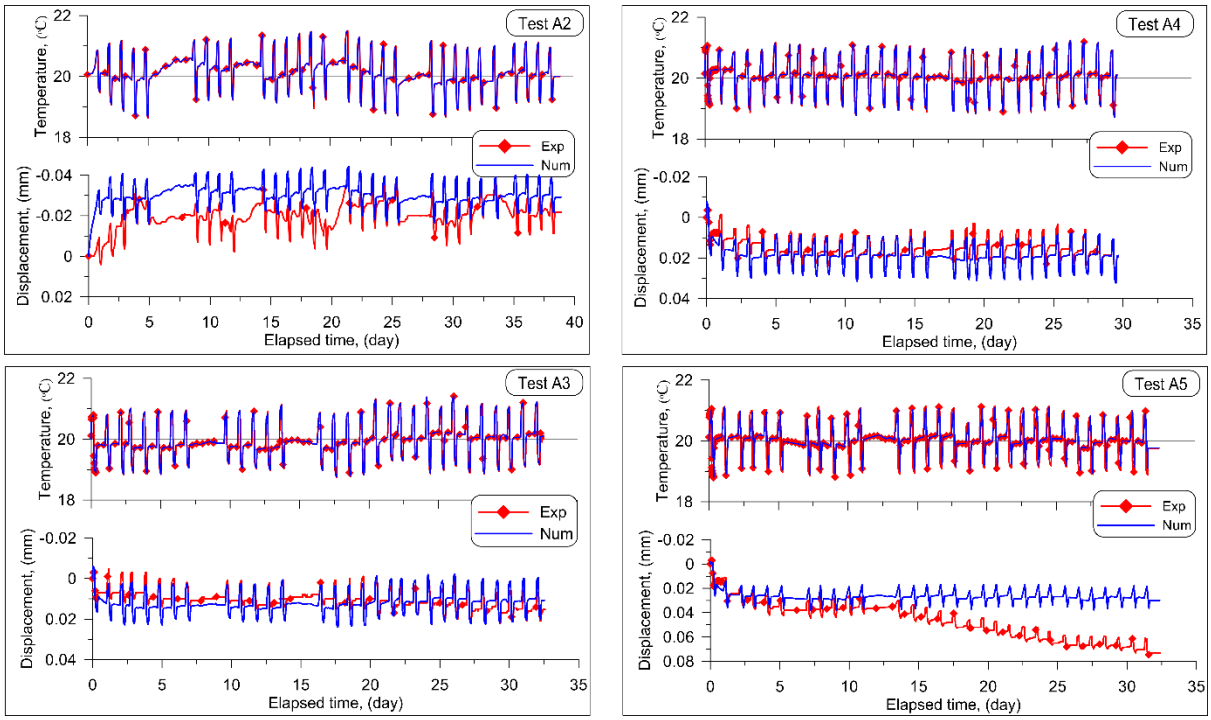

Figure 4.5 Temperature and pile head displacement versus elapsed time (A2–A5)

To better analyse the pile head displacement during each thermal cycle, in Figure 4.6, displacement is plotted versus pile temperature for the first and last cycles only. The free expansion curve, obtained with the assumption of a pile restrained at its toe, is also plotted. In each thermal cycle, heating induces pile head heave and cooling induces pile head settlement. For tests A3, A4 and A5 (under constant head load), the first thermal cycle induces a significant irreversible settlement. For the case of test A2, where no head load was applied, the behaviour during the first thermal cycle is quite reversible. For the last thermal cycle, reversible behaviour

can be observed for all the tests. Besides, it can be noted that the slope of the pile head displacement versus temperature change during the cooling phase is slightly smaller than that of the free expansion curve.

The results obtained by the numerical simulation are generally in agreement with the experimental ones. The behaviour obtained during the last thermal cycle is strictly reversible and the first thermal cycle in tests A3, A4 and A5 (under constant pile head load) induce significant reversible settlement. Only the behaviour of the first cycle of test A2 (without pile head load) show a difference. In the numerical model, an irreversible pile head heave was obtained after the first thermal cycle.

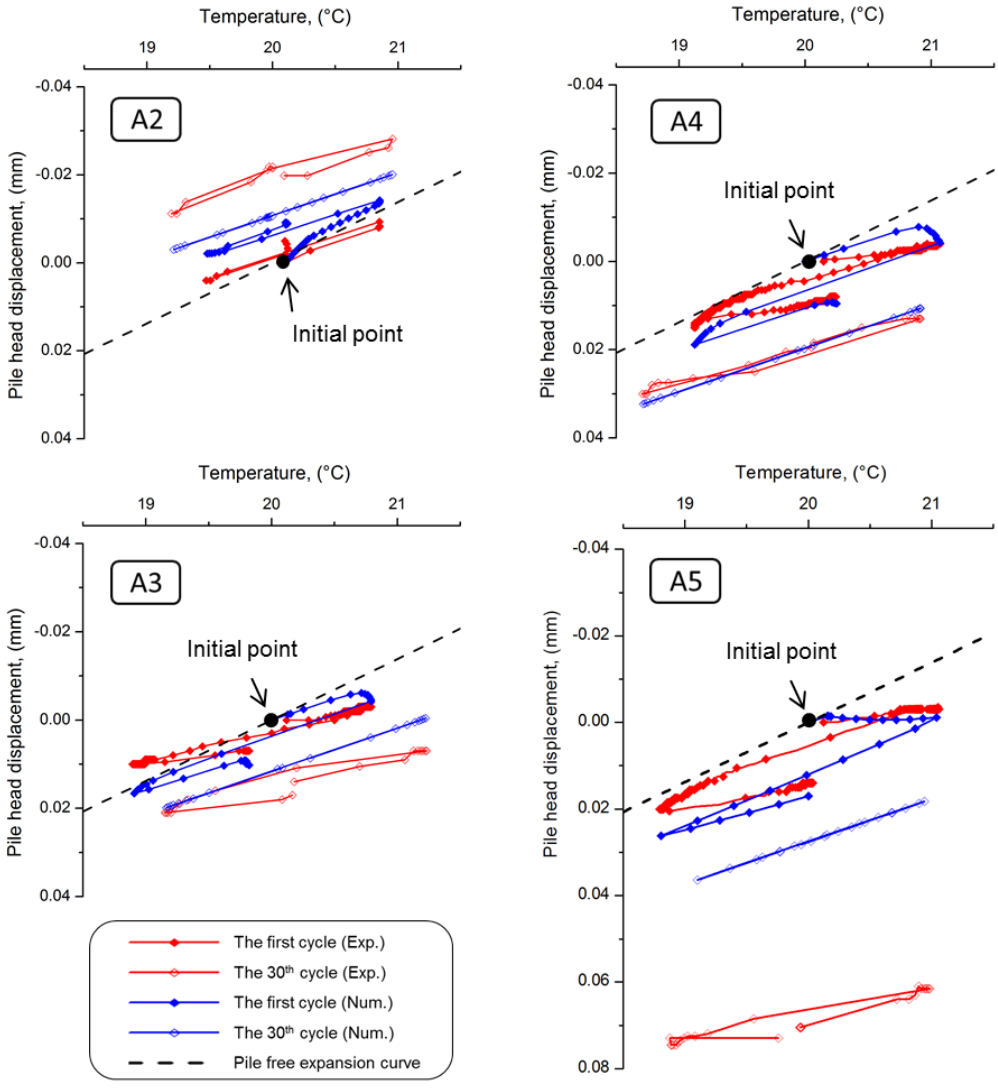

Figure 4.6 Pile head settlement versus pile temperature during the first and 30th cycles

The irreversible pile head displacement is plotted against the number of cycles in Figure 4.7. For a better comparison with full-scale experiments, it is also normalised with the pile diameter. For test A2, the first cycle induces pile head heave up to 0.15% of pile diameter with the numerical model. Afterwards, the pile behaviour remains reversible during thermal cycles. However, with the physical model, the first cycle induces only very small pile heave (0.03% of pile diameter). But pile heave continues to increase during the subsequent cycles and reaches 0.20% of pile diameter after four cycles. For tests A3 and A4, the first thermal cycles induce significant irreversible settlement. This later becomes negligible for the subsequent cycles. The behaviour of the pile in test A5 is also similar to that of tests A3 and A4. However, after the tenth cycle, the irreversible settlement increases continuously with the increase in the number of cycles. Besides, it can be noted that the irreversible settlement depends on the pile head load; the higher the pile head load, the higher the irreversible settlement. For test A5, the sudden increase of irreversible settlement from the 10^{th} cycle could be related to some technical problems that we could not explain.

The results obtained by the numerical simulation are generally in good agreement with the experimental ones. The only difference is related to test A5 where the pile head's irreversible displacement remains constant even after the tenth cycle in the numerical simulation.

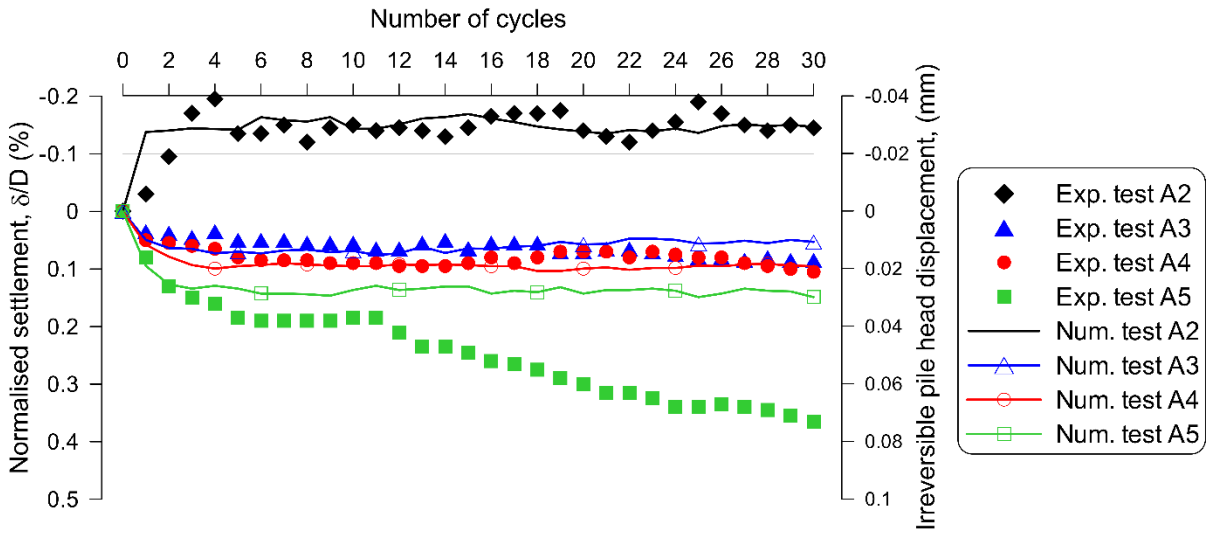

Figure 4.7 Irreversible pile head displacement versus number of thermal cycles

The long-term performance of the pile is further illustrated according to the numerical results. Vertical displacement of pile length in the heating phase (H), cooling phase (C) and reheating phase (R) are plotted in Figure 4.8. The first, second, twentieth and thirtieth thermal cycles are selected here because the simulation results show that the majority of irreversible settlement happens within the first-three cycles and is relatively stable in the rest of the thermal cycles. Note that the vertical displacement of the pile is assumed zero at the beginning of the first cycle in order to be consistent with Figure 4.7. It is obvious that heating and cooling the pile causes displacement distribution to be a mirror-reflection of each other and the vertical displacement remains constant along the pile length in the reheating phase. Displacement shifts to stabilise settlement with thermal cycles continuously. In addition, the null point stabilised at about 430 mm beneath the top surface.

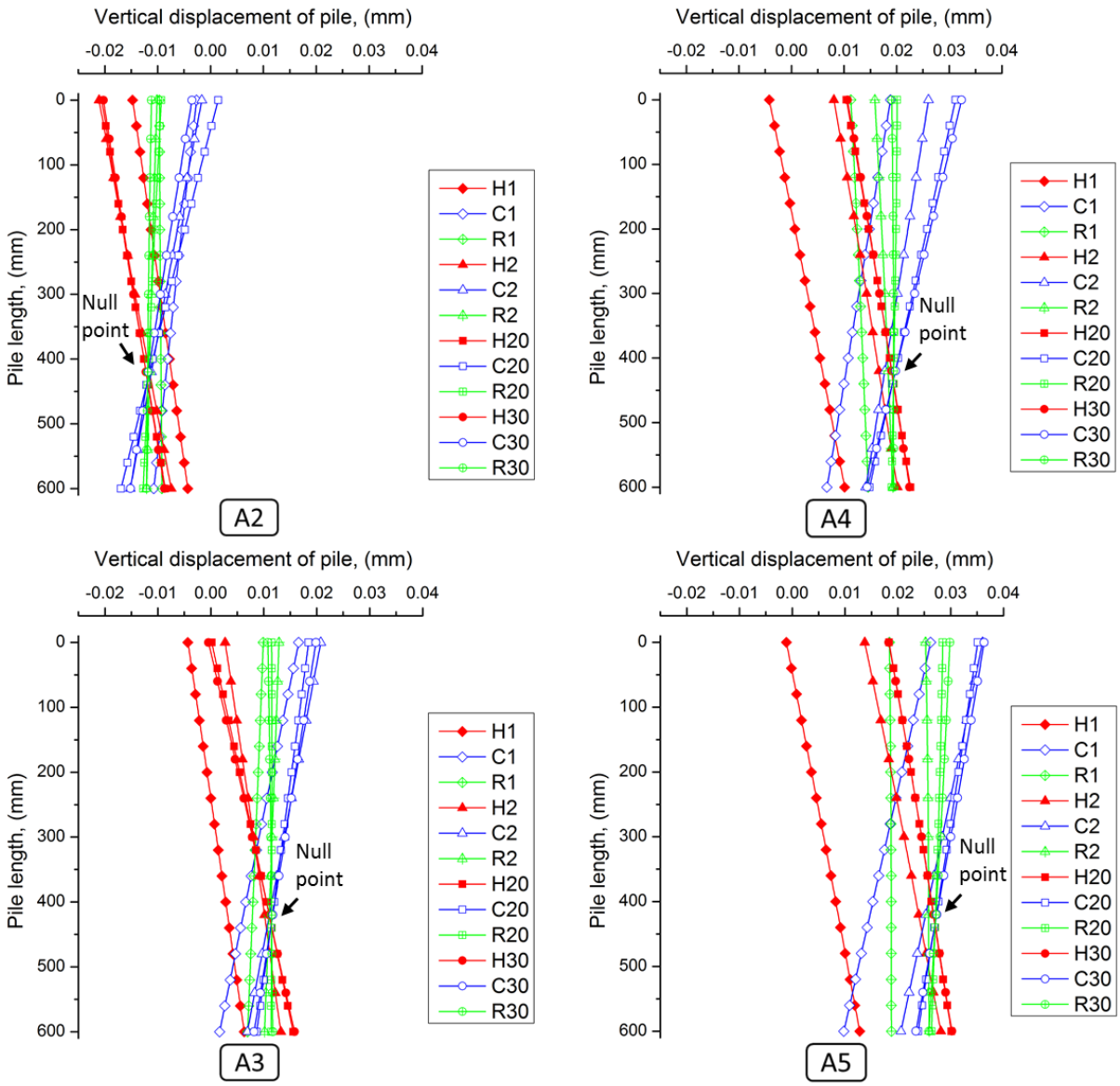

Figure 4.8 Vertical displacement along the pile length (numerical results)

The total vertical stress along the pile length under different thermal cycles obtained from the numerical simulation is presented in Figure 4.9. Only the results obtained from the first and last cycles are presented for clarity. Generally, heating the pile induces a slight increase of vertical stress and cooling causes a decrease in vertical stress distribution along the pile length. The behaviour obtained during the first cycle of test A2 is slightly different; heating induces a decrease of vertical stress and cooling decreases this again later. Besides, the vertical stress is

observed to slightly increase from the first to the last thermal cycles in all heating, cooling and reheating phases.

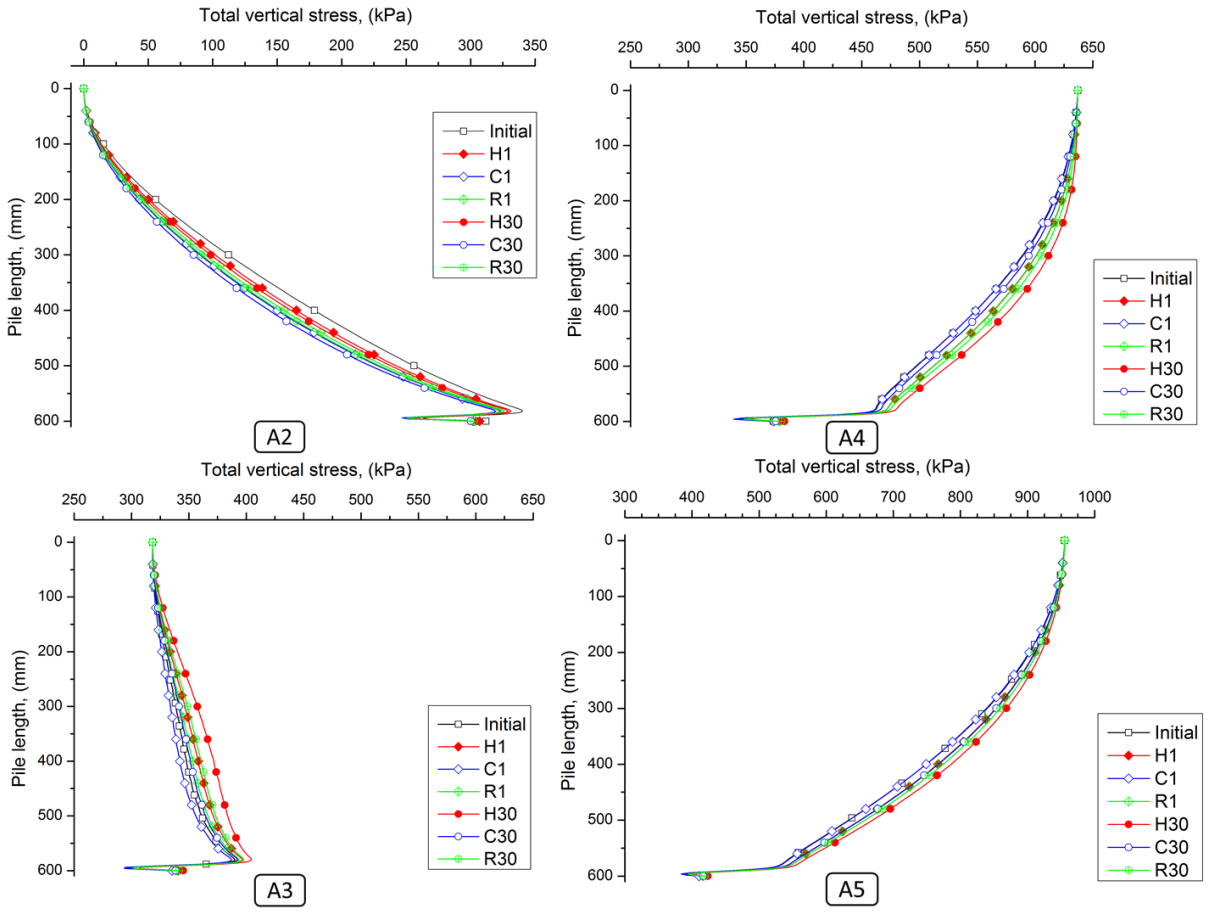

Figure 4.9 Thermal effect on the total vertical stress along the pile length (numerical results)

4.3 Discussion

In the mechanical test paths (test A1), the material parameters for the numerical simulations are adopted from Lv et al. (2017). From the results, it is obvious that the estimated bearing capacity is in agreement with the experimental results (Figure 3.4 in Chapter 3). A carefully estimated lateral stress coefficient (K_0) is important to consider the compaction process in the physical model.

In test A2, the upward displacement of the pile (as shown in Figure 4.5) during heating/cooling cycles, observed on both physical and numerical models, can be explained by the stress state shown in Figure 4.9. Actually, test A2 starts after the mechanical unloading path of test A1. At the end of the unloading path, the pile is still subjected to compressive stress (up to 300 kPa at its toe). Thermal cycles in test A2 induce thermal dilation/contraction of the pile. This movement would release this compressive stress and heave the pile. The results shown in Figure 4.9 are evidence of this stress release after thermal cycles.

In the subsequent tests (A3, A4, A5), irreversible settlement was observed during the first thermal cycles. These results are in agreement with those observed by Ng et al. (2014) (using centrifuge modelling) and Vieira and Maranha (2016) by using the finite element method. However, only five thermal cycles were investigated in these works. Actually, the axial stress profiles plotted in Figure 4.9 show that these thermal cycles increase the axial stress along the pile. This means the thermal dilation/contraction of the pile facilitates the transmission of axial pile head load to the pile toe. In the present works, both numerical and physical models show that the pile settlement becomes reversible under thermal cycles at high numbers of cycles (except for test A5).

The numerical model shows that the behaviour is similar to that obtained by the physical model; the pile settled progressively to achieve a stable state due to the densification process in each thermal cycle. In particular, the first thermal cycle shows good agreement with the experimental results (Figure 4.6). The explanation of why numerical simulation is able to predict progressive settlement is due to the use of the modified Cam-clay model as the constitutive model for soil. The Cam-clay criterion follows the poro-plasticity rule that could more effectively simulate the densification process during thermal cyclic loads; whereas Mohr-Coulomb's model may not well describe such soil behaviour (Yavari et al., 2014a). Therefore,

the present numerical prediction of long-term thermal cyclic settlement of energy piles is able to predict experimental data with relatively good agreement.

The results of Figure 4.6 show that the slope of the pile head displacement versus temperature change during the cooling phase is slightly smaller than that of the free expansion curve. Actually, similar tests on dry sand have shown that this slope is similar to the free expansion curve (Kalantidou et al., 2012; Yavari et al., 2014a). The behaviour observed in the present work can be explained by the results shown in Figure 4.8. Actually, the null point is not located at the pile toe but at a depth of 400–450 mm. For this reason, the pile head displacement does not correspond to the free expansion of the whole pile length.

In the present work, the numerical model was able to correctly reproduce the thermo-mechanical behaviour of a small-scale energy pile under several thermal cycles. Note that the range of the temperature variation in the physical model was limited to ±1 °C. This value is much smaller than the full-scale application (up to ±20 °C) in order to reflect the scale effect. Within this limited range of temperature variation, the soil parameters can be assumed to be independent of temperature. However, for a higher temperature variation, the temperature change can slightly modify the soil properties (Hong et al., 2016; Tang et al., 2008; Yavari et al., 2016a). The use of the present numerical model to predict the behaviour of real-scale energy foundations should consider this aspect.

4.4 Summary

The long-term thermo-mechanical behaviour of energy piles is investigated in the present work by using a small-scale model pile (physical modelling) and the finite element method (numerical modelling). The following conclusions can be drawn:

- Thermal cycles applied to the pile under constant pile head load induce stress redistribution inside the pile. This can induce irreversible pile heave in the case without pile head load, and irreversible pile settlement in the case with pile head load.
- The irreversible pile head settlement/heave is more important within the first thermal cycles; it becomes negligible at high numbers of cycles.
- The main mechanism that controls soil interaction during thermal cycles under constant pile head load is pile thermal contraction/dilation. The numerical model can correctly capture the experimental results without considering temperature effects on the soil's parameters.

The preliminary results shown in this paper could warrant future numerical studies for the serviceability design of geothermal energy piles.

Chapter 5. Thermal Performance Analysis

The importance of geothermal energy pile design is not only considering settlement response under thermal cyclic loading but also investigating the thermal performance behaviour under such long-term cyclic loading. As mentioned in the literature review, the majority of researches focused on thermal performance/response of individual piles by alternating configuration of water circulation pipes or optimising operational techniques to maximise thermal exchange rates, whereas papers mentioning the performance of piles in groupings are rare. This study is based on annual thermal cycles as previous chapter—energy pile mechanism study but has focused on different research aspects — thermal performance in annual thermal cyclic loading conditions. Numerical methods are used and compared with literature for validation purposes. After that, the thermal performance of piles in foundation groupings are investigated.

In this chapter, individual thermal performance of energy piles is reviewed from the literature by a simplified modelling technique, as discussed in Chapter 3, and then the study is extended into pile groups to further investigate this simplified technique. Several grouping pile models are established, with centre-to-centre pile spacings of 1 m and 2 m, to study spacing influences. Typical pile locations of corner pile, edge pile and centre pile were selected to represent all piles in grouping energy pile foundations. Finally, the alternating heating strategy in the pile operation is discussed in terms of thermal heat exchange power and total energy extraction. This study could be used as guidelines for HVAC practice to estimate power reduction rates with total energy demand on buildings.

5.1 Numerical model

This study is modelled by commercial finite element software ABAQUS standard V6.16 heat transfer analysis. A three-dimensional model is used to study the thermal effects that influence the adjacent pile. Figure 5.1 (a), (b) and (c) present finite element mesh for simulating thermal

exchange tests in a single pile and pile groups with the 1 m and 2 m spacing, respectively. Refined mesh near the soil-pile interface is used. Surfaces between the soil and pile are tied together to reduce mesh dependency and ignore the interfacial thermal conductance effect, which means fully thermal conduction occurs across the surface. Thermo-mechanical behaviour, such as expansion and relative interface slip, are ignored in this study. Six node linear heat transfer triangular prism (CD3D6) element type is used for the whole domain and 17 °C is the initial temperature condition applied to the entire domain. Furthermore, the constant temperature of 17 °C and zero heat flux boundary conditions are applied at the lateral and bottom surfaces, respectively. The ground temperature selection is consistent with the range used in many research reports (Bezyan et al., 2015; Faizal et al., 2016; Franco et al., 2016; Gao et al., 2008b; Kramer et al., 2015; Yoon et al., 2015). The closest distance from the heating source to the lateral boundary is greater than 11 times the pile radius for all simulation models in order to avoid the boundary effects according to Ghasemi-Fare and Basu (2013). For simplicity, two layers separate the soil domain instead of three layers in Park et al. (2013), because energy extraction measurement takes place at 4.75 m below the top surface, and unsaturated soil properties have less influence in terms of heat exchange. Properties for soils and piles are summarised in Table 5.1.

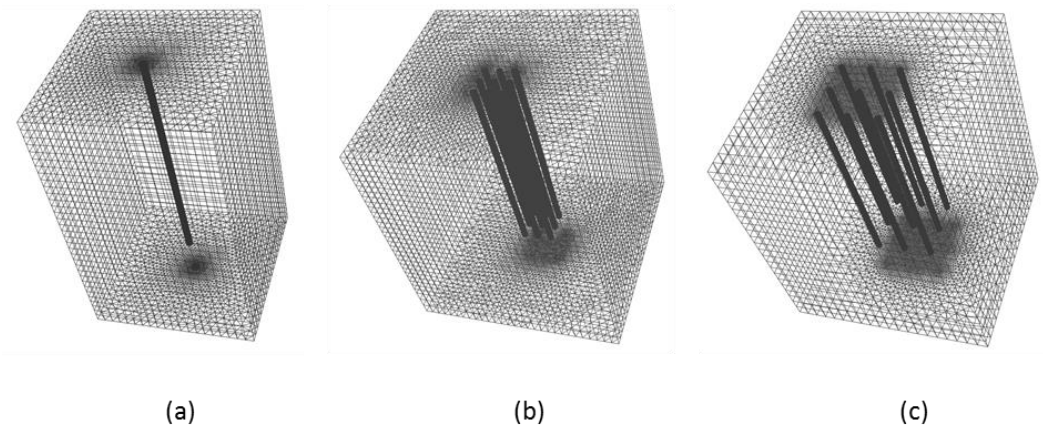

Figure 5.1 FEM mesh of: (a) single pile (b) 9 piles group with pile distance of 1 m, and (c) 9 piles group with pile distance of 2 m

5.2 Model validation

To ensure consistency between the simulation and analytical solutions, line sourced heating at the centre of the pile is applied within a single pile model, and a finite line sourced heating model (Zeng et al., 2002) is used in comparison (Equation 2.2 in Chapter 2). The properties are the same as the analytical method, which means that the thermal properties of the pile are ignored and replaced by soil properties in ABAQUS simulation. Additionally, homogenous soil properties are considered because of limitations of existing analytical models. Properties are referenced to Park et al. (2013) by considering soil layer 2.

Table 5.1 Simulation parameters in thermal performance analysis

	Soil*	Rock	PHC	Grout
Thermal conductivity (W/(m°C)	2.4	3.24	1.62	2.02
Heat capacity (J/kg°C)	2140	823	790	840
Density (kg/m^3)	1280	2640	2700	3640

*soil layer 2 in Park et al. (2013)

Total energy applied in the analytical method is 200 W/m. For simulation, energy is applied per node at the centre to make it equivalent to the line source. There are 275 equal-spacing nodes at the centre and 10 W per node is applied, which is equal to 200 W/m for the 13.75 m length of the pile. Two locations between the analytical and simulation solutions are compared at the radius of the borehole wall (r = 0.2 m) and mid-sections of the soil body (r = 2.544 m) in the mid-height of the pile length (6.875 m). From the methods above, it seems there are no differences in thermal response, which means that line source heating simulation results are consistent with finite line source heating analytical results (Figure 5.2).

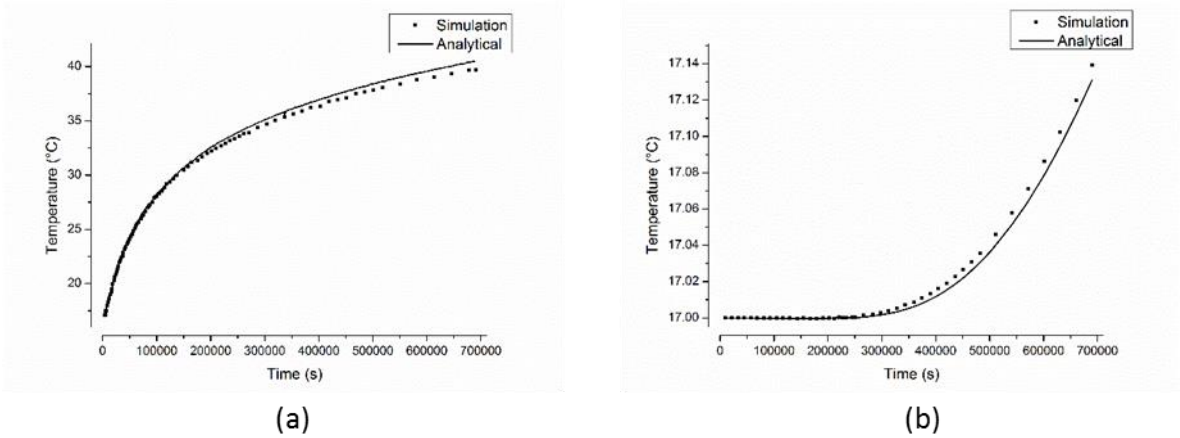

Figure 5.2 (a)Temperature near the borehole wall, mid-height of borehole, r = 0.2 m; and (b) Temperature at middle of soil body, mid-height of borehole, r = 2.544 m

However, if physical properties of concrete are applied to the simulation, due to non-uniform energy output from the grout core to the PHC cover, it is hard to define total energy output in analytical solutions. So, a body heat flux 2750 W along the length of 13.75 m, for the entire pile was applied for simplicity. Also, r = 2.544 m was selected to avoid boundary effects (reasonably away from the pile surface). From the graph, because the distance from the heating source to the selected point has changed, this distance is 2.544 m for the analytical solution and 2.544 m minus 0.2 m (pile radius), therefore differences are observed. This can be explained by the fact that the neglected pile radius in the analytical solution may cause different temperature distributions. The pile radius (0.2 m distance) is deducted from the analytical solution for comparison to ensure that the measurement distance is the same, meaning that the simulation result and the analytical solution are consistent and therefore the simulation model is eligible to further study thermal performance of pile groups (Figure 5.3).

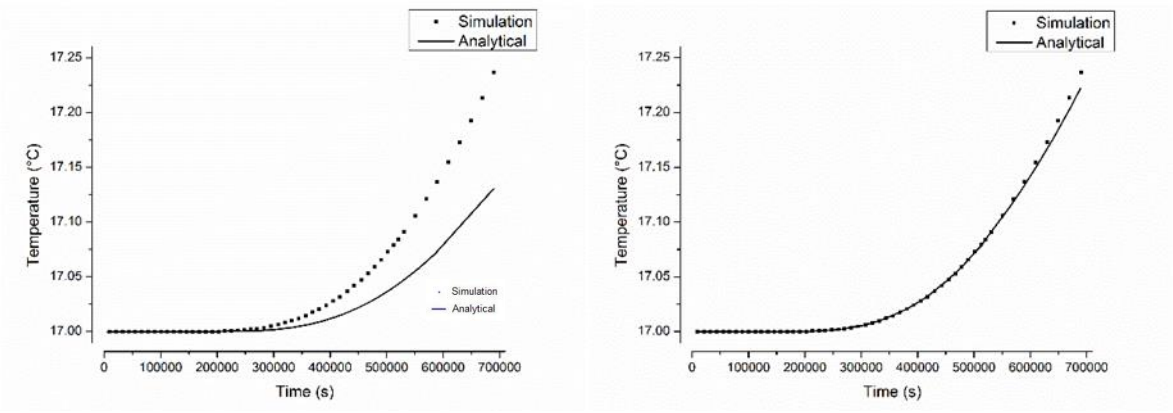

Figure 5.3 Body heat flux simulation vs analytical line source heating: (a) radius at 2.544 m, and (b) deduced radius from analytical solution 2.544 – 0.2 m

Further verification of the simulation model is done by comparing the thermal exchange rate with Park et al. (2013) where different pipe configurations of geothermal energy piles were studied. Here, as mentioned above, comparison of results for the 3U pipe line configuration and the W pipe line configuration are presented in the equivalent heating zone method. It should be noted that only the continuous operation mode is to be used to fit the heating diameter of the equivalent heating zone, whilst the cyclic loading cases are served as predictions from the current model. In the 3U case, a 50-day period is compared (Figure 5.4); and a 90-day period is compared in the W-case (Figure 3.5 in Chapter 3). This simplified method shows good relative agreement in the thermal exchange rate of the continuous operation mode. Moreover, selected point comparison is also presented for intermittent operation mode in the 3U pipe configuration case in Figure 5.4. Two typical points are chosen for each heating cycle: instantaneous maximum thermal exchange rate and shoulder thermal exchange rate (when fluid circulation stops). Because of different heating techniques on the energy pile, the maximum thermal exchange rate in the current equivalent heating zone boundary method is larger than the nodal convective heat boundary method. It can be explained by more instantaneous accuracy of modelling of fluid temperature inside the circulation pipe in the first few seconds which influences maximum thermal exchange rate significantly. In the proposed model, this

can be also captured if a ramp of temperature instead of a temperature jump is applied to the equivalent heating zone, however, this requires another model parameter for representing the characteristic heating time and will not be discussed here.

From an energy exchange point of view, such differences can be ignored because it would not significantly influence total energy absorption by a time integration. With time in operation, the equivalent heating zone method appears to be consistent, in particular the shoulder thermal exchange rate is almost the same for both modelling methods. From the comparison of two approaches above, it is found that the equivalent heating zone boundary method is capable of studying thermal performance in geothermal energy piles.

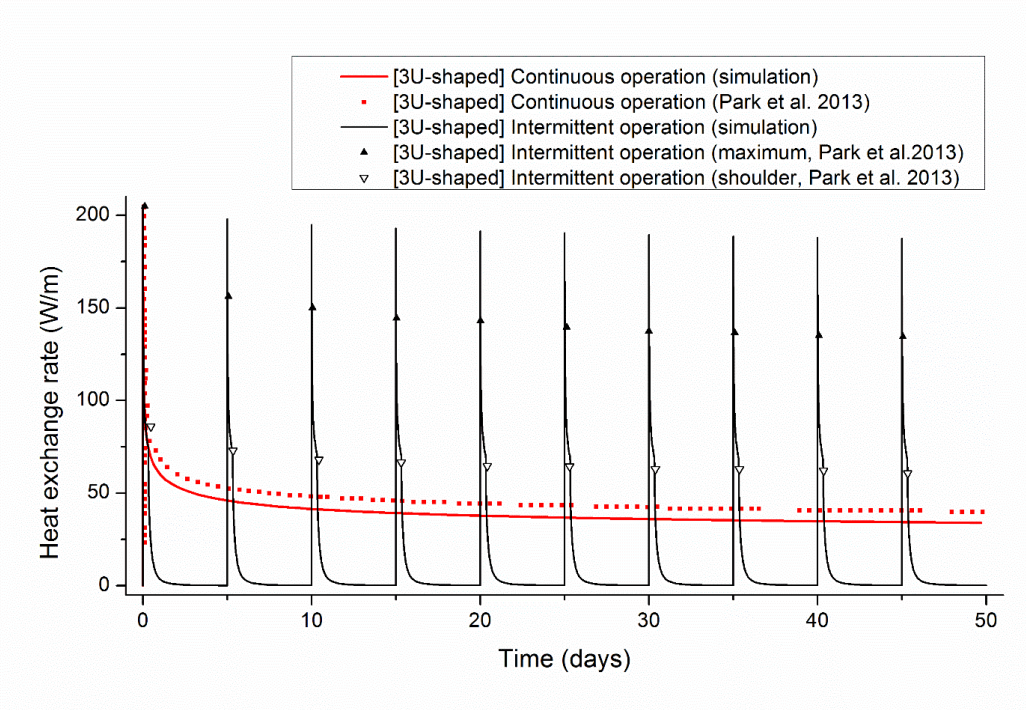

Figure 5.4 Heat exchange rate comparison between the simulation results (lines) and 3U-pipe cases of Park et al. (2013) (dots).

5.3 Results and discussion

Cumulative energy extraction can be calculated by integration of heat exchange rate over time. In this study, by doing temperature control, total heat flux over the pipe surface is obtained and integrated with time to get cumulative energy extraction. An intermittent operation mode within an 8-hour period is considered. The energy extraction can be estimated using the following equation:

$$Q = \sum_{i=1}^{i} \frac{(t_{i+1} - t_i)(p_i + p_{i+1})}{2} \quad , \qquad 5.1$$

where Q is the cumulative heat energy below 4.75 m, t is the time, i is the increment number, p is total heat flux through the PHC and grout interface below 4.75 m. Cumulative energy over time for different pile locations and distances is presented in Figure 5.5.

Selected thermal cycles, 1st, 5th 10th, 15th and 20th, are shown here for clear presentation. Generally, the first cycle of energy pile in the same location has less influence in the heat exchange by pile spacing; all typical locations from the energy extraction perspective are equivalent to the first cycle of a single pile which is about 10.7 kWh with 8 hours of operation. Cumulative energy from a long-term perspective tends to be linear with time, but the first few hours increase slightly rapidly compared with the overall trend since the instant thermal exchange rate highly depends on time when the operation initially starts. Group piles with narrower spacings (1 m) reduce their absorbed energy increment quicker than the ones with wider spacings (2 m), as expected from comparison between the 1 m and 2 m spacings for Piles #1, #2 and #5. The wide spacing (2 m) pile foundation shows less sensitivity to thermal cyclic loads. The cumulative energy after several cyclic heating is still maintained relative higher absorption amount in wide spacing case where energy absorption in closer spacing case is lower after several thermal cycles, namely, wider centre-to-centre pile spacing stabilised quicker at higher energy absorption levels because of less thermal influence in the zone. For

instance, Pile #1 with a spacing of 1 m drops by 36.2% of total energy extraction, but for the same location at a far spacing of 2 m, the drop is 23.5% from the 1st cycle to the 20th cycle. For all piles under the same foundation, the corner pile (Pile #1) reaches the highest steady-state energy absorption since it only has thermal influence from two edges. This is followed by the edge pile (Pile #2) that has thermal influence from three edges, and then the lowest energy absorption occurs at the centre pile (Pile #5), which is surrounded by 8 piles from four edges. This geometrical arrangement could explain the reduction of energy absorption from different pile locations. Table 5.2 shows the percentage of energy reductions due to thermal cycles individually. Overall, pile groups with closer spacings that reduce total energy exchange should be considered in HVAC practice.

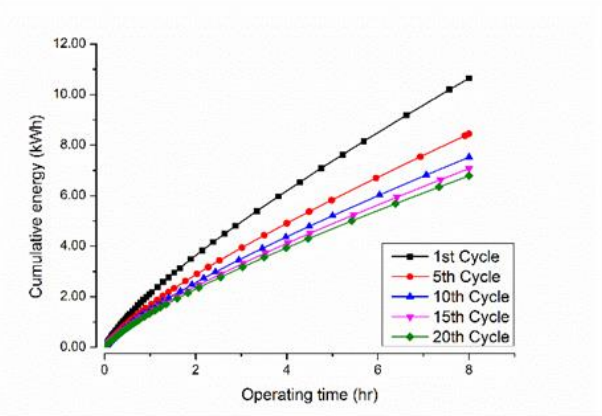

(a) Pile #1, 1 m spacing

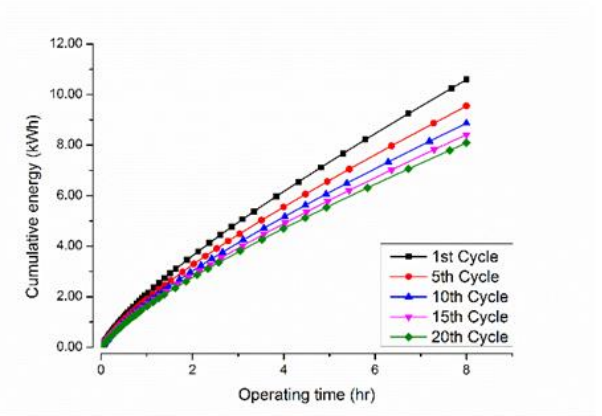

(d) Pile #1, 2 m spacing

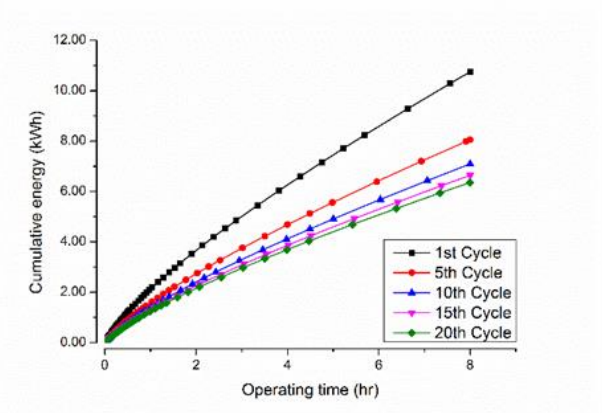

(b) Pile #2, 1 m spacing

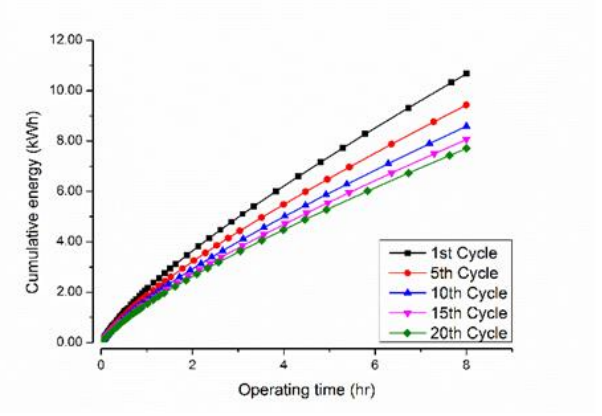

(e) Pile #2, 2 m spacing

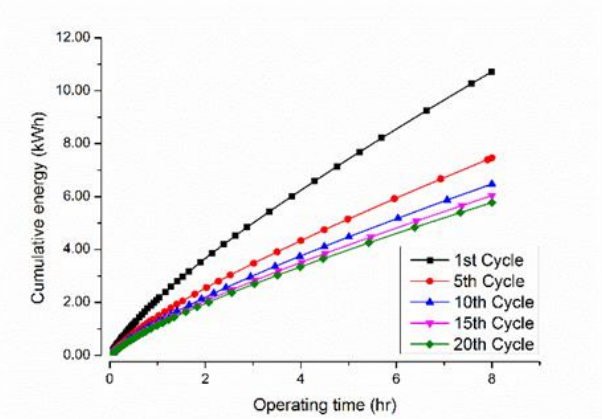

(c) Pile #5, 1 m spacing

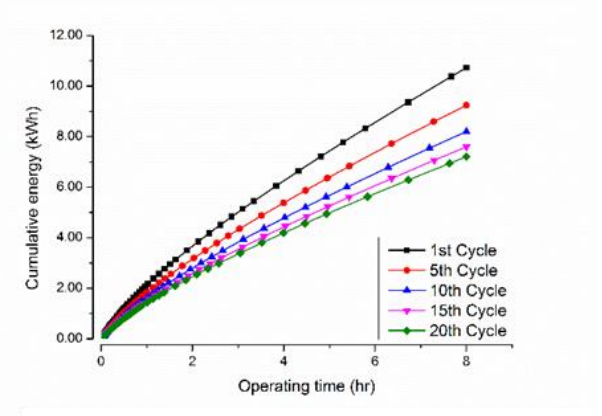

(f) Pile #5, 2 m spacing

Figure 5.5 Cumulative energy over time for different pile locations and distances

Table 5.2 Percentage of energy reduction at steady-state (after 20th operation cycles) due to thermal cycles

Pile spacing/location	1 m	2 m
Pile #1 (corner)	36.2%	23.5%
Pile #2 (edge)	40.8%	27.7%
Pile #5 (centre)	46.1%	32.8%

The average power over operation duration reflects the thermal efficiency and performance of geothermal energy piles. From analysis of energy absorption above, the average power can be calculated by:

$$P = \frac{\text{cumulative energy}(J)}{\text{operating time}(s)} \ , \qquad 5.2$$

Even though the instant heat exchange rate drops significantly during the intermittent operation mode as shown in Figure 5.4, the average power for a certain operation duration may not be significantly influenced by thermal cycles. Figure 5.6 plots single pile average power during 8 hours of operation after cycles as a reference; it shows an insignificant power decrease because total energy absorption stays at a relatively constant level in single pile power study. Given the definition that change of less than 1% can be considered as a relative steady state, the single pile that can be considered to have infinite spacing, reaches it steady-state after the 3rd cycle where 1.23 kW heat extraction power was observed. This agrees with the 1.196 kW cooling capacity found by Park et al. (2013).

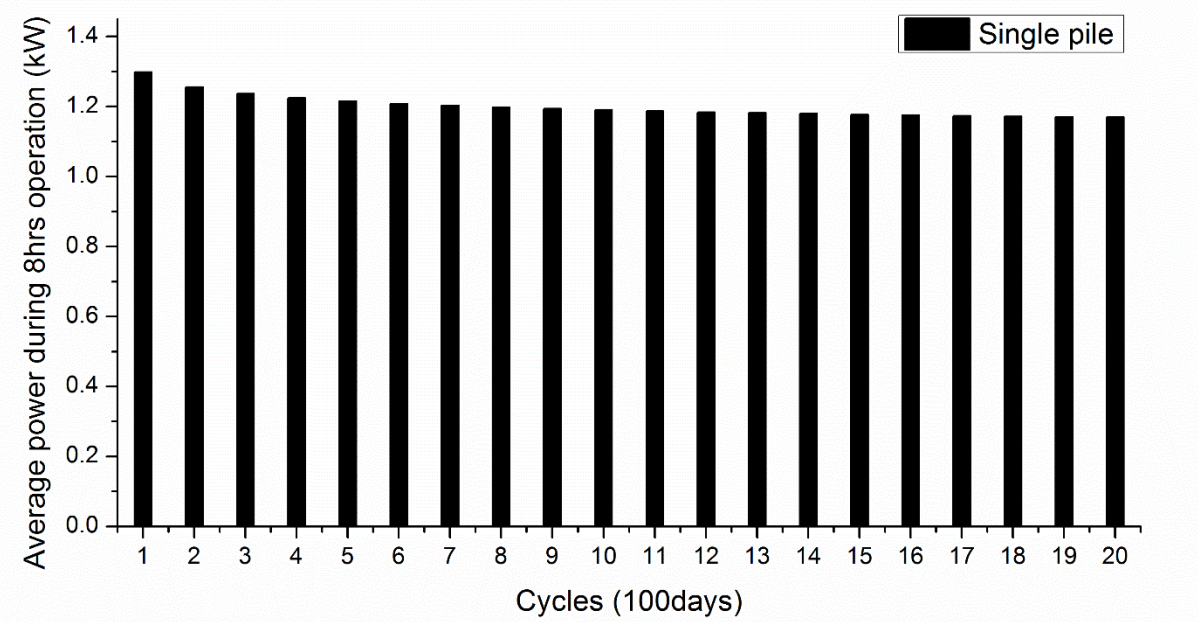

Figure 5.6 Average power during 8 hours of operation (single pile)

As a group pile, centre-to-centre spacing plays a vital role in geothermal energy pile performance. Piles in the same location but in different spacings are compared in Figure 5.7. Corner Pile #1, with two thermal influence edges, has the quickest tendency to reach steady-state thermal exchange power, but it is still relatively slow to reach a steady state with closer centre-to-centre spacings. For example, Corner Pile #1 with a 1 m spacing stabilises after the 16th cycle, corresponding to 0.875 kW cooling power; and the 2 m spacing pile reaches stability after the 13th cycle, with 1.070 kW cooling power. The power difference at stabilisation between the two spacing is 18.2%. A similar trend appears for Edge Pile #2 where the power generation for the 1 m spacing in steady state is 0.820 kW at the 16th cycle and 0.997 kW for the 2 m case at the 16th cycle. Furthermore, Centre Pile #5, which is surrounded by 8 piles, has the slowest tendency to reach stability and stays at 0.746 kW and 0.918 kw for the 1 m and 2 m cases at the 16th and 19th cycles, respectively. To summarise, in HVAC engineering practice, individual geothermal pile energy performance is based on the pile location and designed centre-to-centre pile spacing. The results show that closer spacing with larger thermal influence edges lowers cooling power and also extends stability cycles.

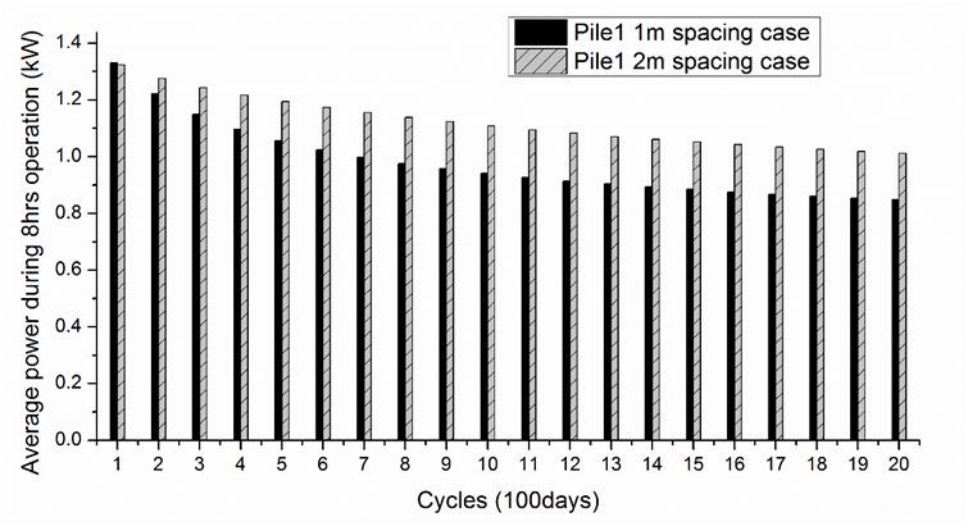

(a) Corner Pile #1

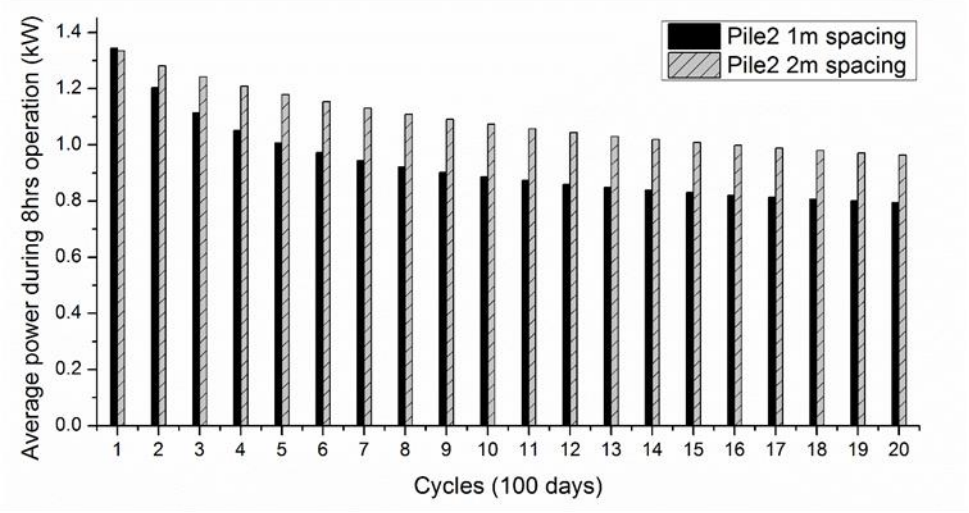

(b) Edge Pile #2

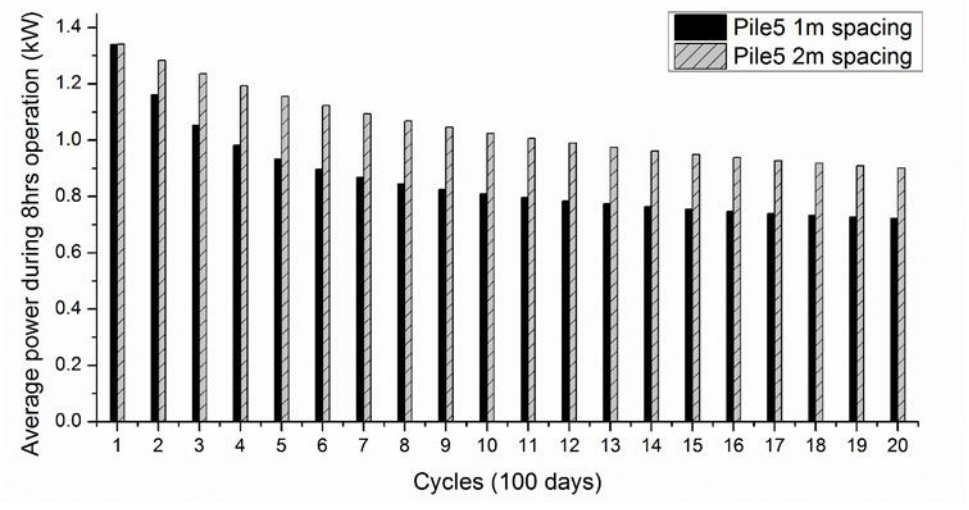

(c) Centre Pile #5

Figure 5.7 Power comparison between two different spacings: (a) Corner pile (Pile #1), (b) Edge pile (Pile #2), and (c) Centre pile (Pile #5)

Further analyses were carried out on the relationship among the parameters of cooling power, centre-to-centre spacing and pile location. Single pile cooling power at steady-state was set as the reference because it can be treated as an infinite centre-to-centre spacing with no adjacent pile. The adjacent pile effect could be summarised into three typical cases if the pile group is in a lattice configuration as discussed above. The normalised parameter can be defined as:

$$\text{Power reduction} = \frac{\text{subject pile power}}{\text{reference pile power}} \tag{5.3}$$

$$\text{Normalised distance} = \frac{\text{minimum pile spacing requirement}}{\text{subject pile spacing}} \tag{5.4}$$

From the equations above, the x and y axis limits are 1 because no cooling power from pile grouping would excess single pile power, and no distance would be closer than the minimum pile spacing construction requirement (here equalling 1 m), so an envelope of energy pile maximum performance in the pile grouping can be established. The relationship between power reduction and normalised distance is plotted in Figure 5.8. Thermal impacted faces contributed to cooling power reduction of the energy pile location. The pile's cooling performance under the same spacing distance drops by increasing the thermal impact faces, which means that the corner piles may have a relatively higher cooling power during operation, and the inner pile located in the group has relatively lower cooling power. This result could influence the HVAC designer to arrange a better operating strategy to ensure optimisation of geothermal pile thermal performance.

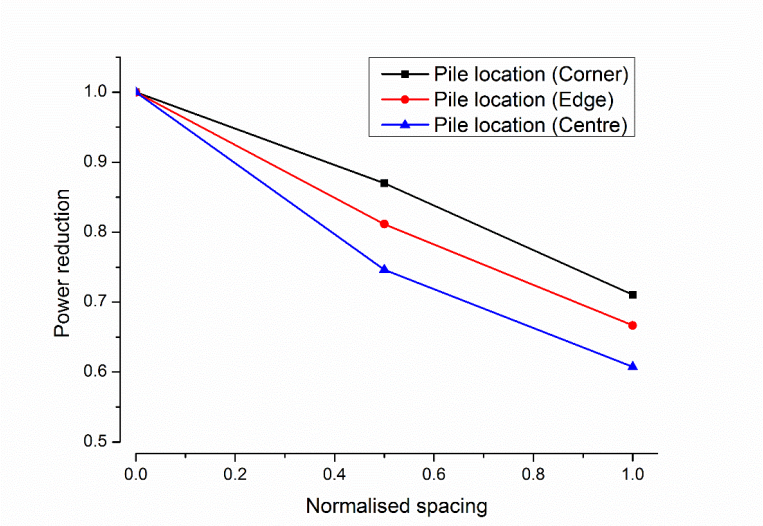

Figure 5.8 Steady-state power envelope

Moreover, we analysed a simple alternating heating operation to give a basic idea for optimising the cooling power of a geothermal energy pile. Figure 5.9 shows the averaged power in a group for the heating strategy studied; where (a) plots four to five piles alternating heating in 2.5 days, and (b) plots four to five piles alternating heating in 5 days. Note that four piles in operation at singular cycles and five piles in operation at even cycles is as mentioned in the model design concept in Section 3.2. The power decreasing in strategic heating after each cycle is considerably lower than the nine piles in the simultaneous heating condition. This is expected because it avoids large amounts of heat injection into the ground at the same time. The average power per pile for five piles is almost equal to the one for four piles after the 11^{th} cycle.

In the 2.5-day thermal cycle case (Figure 5.9a), because it injected the same amount of heat as a fully operational mode during the same period, considering four piles after the 15^{th} cycle as a steady-state matches the corner pile cases. The equivalent centre-to-centre spacing is $2\sqrt{2}$ m for the 2 m case or $\sqrt{2}$ m for the 1 m case. The power reduction ratio from Figure 5.7 can be linearly interpolated as 0.91 for the 2 m case and 0.8 for the 1 m case, where maximum steady-state power is 1.23 kW, so the estimation of average power by calculation are 1.12 kW and 0.98 kW. The simulation results obtained are 1.11 kW and 0.92 kw for the 2 m and 1 m cases,

respectively. This shows that the envelop could give a relatively good hint on estimating pile working power. However, in the 5-day thermal cycle cases (Figure 5.9b), the power reduction is much smaller than expected. It is due to heat injection into the ground in unit time which is lower than other cases in this study. Ground temperature distribution and the recovery process may allow the energy pile to reach higher cooling power. Further study is needed by considering the thermal cyclic period to develop a comprehensive understanding of the power reduction envelope.

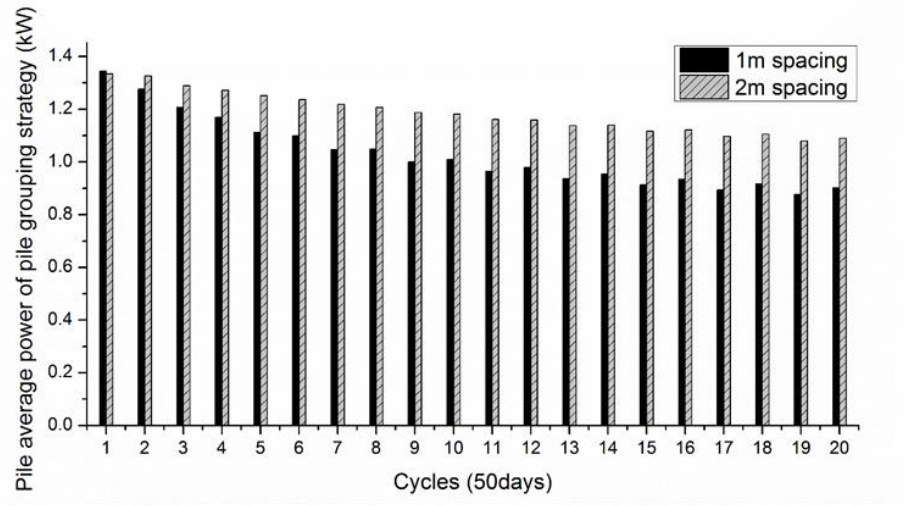

(a)

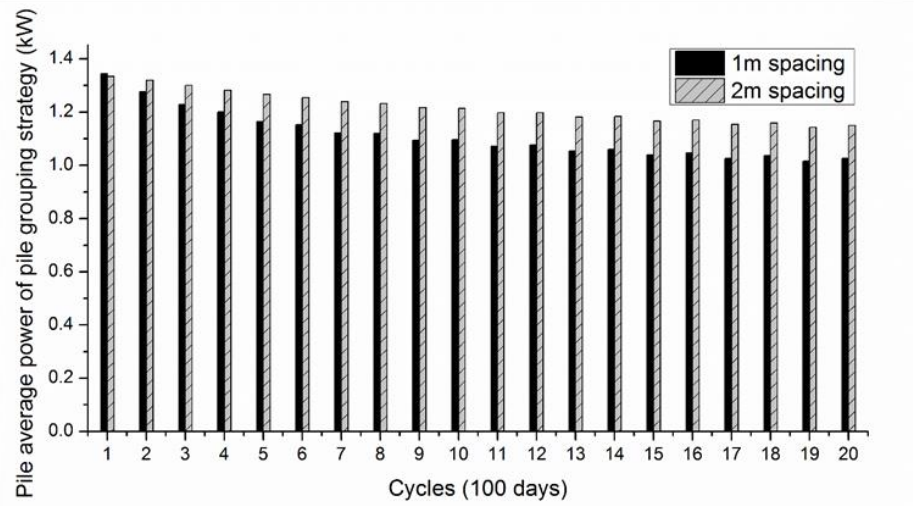

(b)

Figure 5.9 Pile average power per pile of alternating grouping heating: (a) 2.5-day thermal cycle and (b) 5-day thermal cycle

Energy extraction per operation cycle from the ground in 5 days cyclic period between all pile heating and the introduced alternating heating strategy are shown in Figure 5.10. The figure compared full piles operation mode and strategy heating mode for two different spacing, one complete cycle in strategy heating mode contains two 2.5 days alternate heating cycles to ensure consistency with all pile operation mode for entire foundation is heated by 9 piles. It is obvious that dense spacing leads to less energy extraction from the ground after several cycles, wider spacing slows this effect and a relatively higher energy extraction rate is maintained. In terms of different alternated heating period, the group piles are subtracted same amount of energy as fully operation mode within same the time frame. The slight differences between the 2 m spacing operational technique may be due to acceptable error allowance in the finite element method. As a result, thermal efficiency in individual pile is larger for strategy heating but the total energy demand for buildings may not be affected by applying the alternate heating technique within the same operational period.

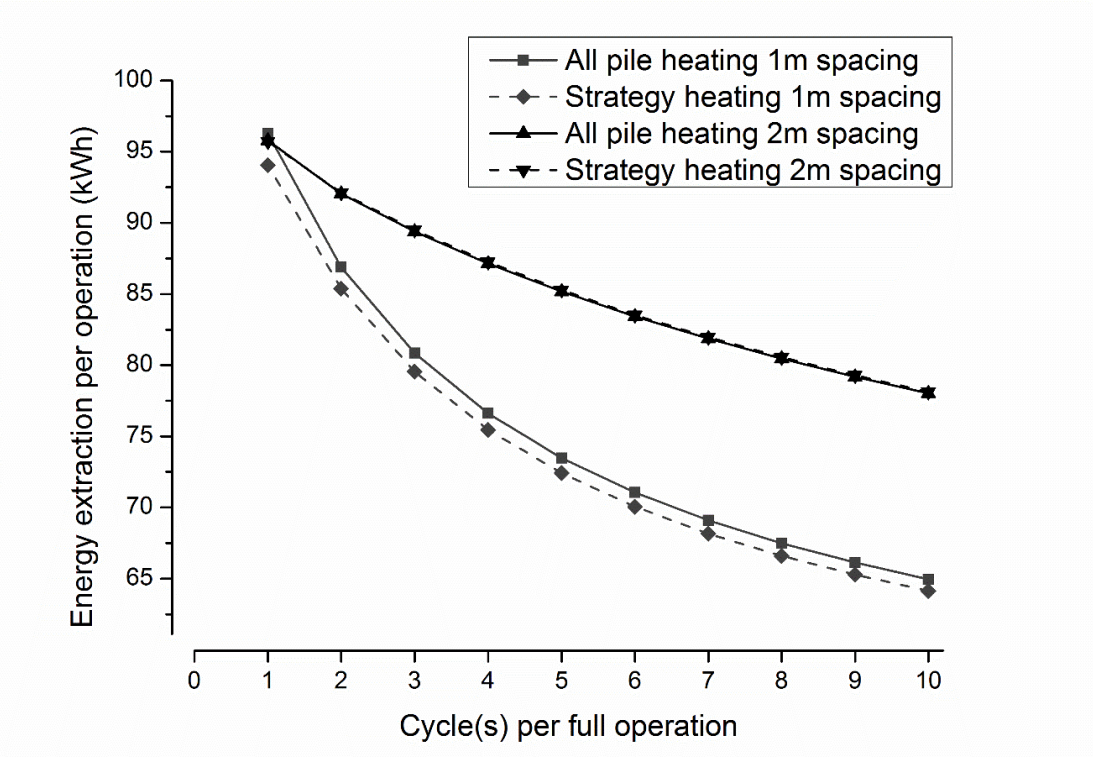

Figure 5.10 Energy extraction per operation cycle from ground over time

5.4 Summary

The thermal performance of energy pile groups is examined in this Chapter. The simulation results of single pile are validated by references and analytical solution. Energy pile thermal performance in cyclic thermal loads can be divided into three different location influences. The following conclusions based on this numerical study can be highlighted:

- Thermal exchange rate is significantly affected by pile centre-to-centre spacing. Narrower spacing with larger thermal influence edges results in not only lower cooling power but also extends the number of cycles to reach stability.
- The corner pile may have a relatively higher cooling power during operation, and the inner pile located in the group has relatively lower cooling power.
- Thermal efficiency in individual pile is larger for strategy heating but total energy demand for buildings may not be affected by applying the alternate heating technique within the same operational period.

This study can serve as an initial step towards HVAC practice to estimate the power reduction rate with total energy demand on buildings. Further study is needed to focus on the recovery period to give a clearer picture of the power reduction relationship of geothermal energy piles.

Chapter 6. Conclusion & Future Work

In this work, geothermal energy piles have been modelled by the finite element method, focusing on two major aspects for long-term operation are: (1) thermo-mechanical behaviour and (2) thermal performance. From energy pile construction and design practice, the energy pile is subjected to thermal cyclic loading conditions in annual operation so the stability and serviceability for the pile as a structural component is very important. This study first presented the thermo-mechanical analysis of the pile under such cyclic loading conditions, which can be compared with a small-scale physical experiment. Furthermore, thermal performance of piles in group foundation is also modelled to investigate the power reduction in relation to pile spacing and pile locations. A simple heating strategy with alternating heating pile groups is introduced to maximise individual pile thermal exchange power.

In the first approach, the thermo-mechanical responses under cyclic loadings are investigated, including settlement, vertical displacement and vertical stress. Pile head settlement changes with applied temperature variation, and the initial few thermal cycles contributed most of the irreversible settlement in this study due to stress redistribution along the pile depth. The finite element simulation is capable of capturing the mechanics by controlling heating and cooling cycles. The study presented a general overview with respect of the mechanical behaviour and heat exchange behaviour of geothermal energy piles.

The study moved further to thermal performance of pile groups under heating cycles. Different pile centre-to-centre spacing in different pile installation locations were investigated. Thermal exchange rate drops and approaches its steady-state condition after applying heating/cooling cycles. Adjacent piles with short distance have negative influence on the thermal exchange rate. Also, different pile locations in pile group foundations influence the pile cooling power. It provides a relationship of power reduction, location and adjacent pile distances. The strategic

heating with alternating operating pile groups shows it would increase individual pile working power, but total energy extraction remains almost unchanged under the same operational period.

In the future, several studies could be considered to further the development of geothermal energy piles and motivate regulation of relevant requirements of geothermal energy pile application and industrialisation.

- A similar test should be conducted in full-scale in-situ experiments to examine the scale factor accuracy. A parallel finite element analysis should be also carried out to examine the dominate factors at the full scale. In particular, at larger temperature variation at the full scale, the thermo-mechanical coupled constitutive model in soil may affect settlement behaviour of energy piles in simulation. Moreover, in-situ experiments of group pile foundations are necessary to investigate the foundation settlement response from a geotechnical design perspective.
- With a high temperature gradient, thermal-driven moisture migration within a soil body may result in a non-uniform thermal conductivity. Combined with a thermo-active constitutive model, greater accuracy in prediction of energy pile mechanisms could be achieved.
- The operational period for thermal performance analysis, namely, the recovery period on the energy pile, is also an important factor in thermal power generation. It should be considered in future to have a full understanding of the power reduction relationship. Power reduction estimation may need multiple pile distances and geometrical arrangement to obtain comprehensive relationships.

References

AFNOR (1999) Essai statique de pieu isolé sous un effort axial, NF P 94-150-1, 28 pages.

Akrouch, GA, Sánchez, M & Briaud, J-L 2014, 'Thermo-mechanical behavior of energy piles in high plasticity clays', *Acta Geotechnica,* vol. 9, no. 3, pp. 399-412.

Amatya, B, Soga, K, Bourne-Webb, P, Amis, T & Laloui, L 2012, 'Thermo-mechanical behaviour of energy piles', *Géotechnique,* vol. 62, no. 6, pp. 503.

Baycan, S, Haberfield, C, Chapman, G, Wang, B, Bouazza, A, Singh, R & Barry-Macaulay, D 'Field investigation of a geothermal energy pile: Initial observations', Proceedings of the 18th international conference on soil mechanics and geotechnical engineering, Paris, France, pp. 2-6.

Bezyan, B, Porkhial, S & Mehrizi, AA 2015, '3-D simulation of heat transfer rate in geothermal pile-foundation heat exchangers with spiral pipe configuration', *Applied Thermal Engineering,* vol. 87, pp. 655-668.

Bodas Freitas, T, Cruz Silva, F & Bourne-Webb, P 'The response of energy foundations under thermo-mechanical loading', Proceedings of 18th international conference on soil mechanics and geotechnical engineering, Comité Français de Mécanique des Sols et de Géotechnique Paris, France, pp. 3347-3350.

Bourne-Webb, P, Amatya, B, Soga, K, Amis, T, Davidson, C & Payne, P 2009, 'Energy pile test at Lambeth College, London: geotechnical and thermodynamic aspects of pile response to heat cycles', *Géotechnique,* vol. 59, no. 3, pp. 237-248.

Brandl, H 2006, 'Energy foundations and other thermo-active ground structures', *Geotechnique,* vol. 56, no. 2, pp. 81-122.

Carotenuto, A, Marotta, P, Massarotti, N, Mauro, A & Normino, G 2017, 'Energy piles for ground source heat pump applications: comparison of heat transfer performance for different design and operating parameters', *Applied Thermal Engineering,* vol. 124, pp. 1492-1504.

Carslaw, H & Jaeger, J 1959, *Conduction of heat in solids: Oxford Science Publications*, Oxford, England.

Dai, L, Shang, Y, Li, X & Li, S 2016, 'Analysis on the transient heat transfer process inside and outside the borehole for a vertical U-tube ground heat exchanger under short-term heat storage', *Renewable Energy,* vol. 87, pp. 1121-1129.

Di Donna, A & Laloui, L 2015, 'Numerical analysis of the geotechnical behaviour of energy piles', *International journal for numerical and analytical methods in geomechanics,* vol. 39, no. 8, pp. 861-888.

Di Donna, A, Loria, AFR & Laloui, L 2016, 'Numerical study of the response of a group of energy piles under different combinations of thermo-mechanical loads', *Computers and Geotechnics,* vol. 72, pp. 126-142.

Dupray, F, Laloui, L & Kazangba, A 2014, 'Numerical analysis of seasonal heat storage in an energy pile foundation', *Computers and Geotechnics,* vol. 55, pp. 67-77.

Faizal, M, Bouazza, A & Singh, RM 2016, 'An experimental investigation of the influence of intermittent and continuous operating modes on the thermal behaviour of a full scale geothermal energy pile', *Geomechanics for Energy and the Environment,* vol. 8, pp. 8-29.

Franco, A, Moffat, R, Toledo, M & Herrera, P 2016, 'Numerical sensitivity analysis of thermal response tests (TRT) in energy piles', *Renewable energy,* vol. 86, pp. 985-992.

Gao, J, Zhang, X, Liu, J, Li, K & Yang, J 2008a, 'Numerical and experimental assessment of thermal performance of vertical energy piles: an application', *Applied Energy,* vol. 85, no. 10, pp. 901-910.

Gao, J, Zhang, X, Liu, J, Li, KS & Yang, J 2008b, 'Thermal performance and ground temperature of vertical pile-foundation heat exchangers: A case study', *Applied Thermal Engineering,* vol. 28, no. 17-18, pp. 2295-2304.

Ghasemi-Fare, O & Basu, P 2013, 'A practical heat transfer model for geothermal piles', *Energy and Buildings,* vol. 66, pp. 470-479.

Hong, PY, Pereira, J-M, Cui, YJ & Tang, AM 2016, 'A two-surface thermomechanical model for saturated clays', *International Journal for Numerical and Analytical Methods in Geomechanics,* vol. 40, no. 7, pp. 1059-1080.

Ingersoll, L 1954, ' Heat conduction with engineering, geological and other applications', New York, McGraw-Hill.

Kalantidou, A, Tang, AM, Pereira, J-M & Hassen, G 2012, 'Preliminary study on the mechanical behaviour of heat exchanger pile in physical model', *Géotechnique,* vol. 62, no. 11, pp. 1047-1051.

Kramer, CA, Ghasemi-Fare, O & Basu, P 2015, 'Laboratory thermal performance tests on a model heat exchanger pile in sand', *Geotechnical and Geological Engineering,* vol. 33, no. 2, pp. 253-271.

Laloui, L, Moreni, M & Vulliet, L 2003, 'Comportement d'un pieu bi-fonction, fondation et échangeur de chaleur', *Canadian Geotechnical Journal,* vol. 40, no. 2, pp. 388-402.

Laloui, L, Nuth, M & Vulliet, L 2006, 'Experimental and numerical investigations of the behaviour of a heat exchanger pile', *International Journal for Numerical and Analytical Methods in Geomechanics,* vol. 30, no. 8, pp. 763-781.

Li, M & Lai, AC 2012, 'Heat-source solutions to heat conduction in anisotropic media with application to pile and borehole ground heat exchangers', *Applied Energy,* vol. 96, pp. 451-458.

Loria, AFR, Gunawan, A, Shi, C, Laloui, L & Ng, CW 2015, 'Numerical modelling of energy piles in saturated sand subjected to thermo-mechanical loads', *Geomechanics for Energy and the Environment,* vol. 1, pp. 1-15.

Lv, Y, Ng, CWW, Lam, S, Liu, H & Ma, L 2017, 'Geometric Effects on Piles in Consolidating Ground: Centrifuge and Numerical Modeling', *Journal of Geotechnical and Geoenvironmental Engineering,* vol. 143, no. 9, pp. 04017040.

Man, Y, Yang, H, Diao, N, Liu, J & Fang, Z 2010, 'A new model and analytical solutions for borehole and pile ground heat exchangers', *International Journal of Heat and Mass Transfer,* vol. 53, no. 13-14, pp. 2593-2601.

Mimouni, T & Laloui, L 2014, 'Towards a secure basis for the design of geothermal piles', *Acta Geotechnica,* vol. 9, no. 3, pp. 355-366.

Miyara, A, Tsubaki, K, Inoue, S & Yoshida, K 2011, 'Experimental study of several types of ground heat exchanger using a steel pile foundation', *Renewable Energy,* vol. 36, no. 2, pp. 764-771.

Murphy, KD, Mccartney, JS & Henry, KS 2015, 'Evaluation of thermo-mechanical and thermal behavior of full-scale energy foundations', *Acta Geotechnica,* vol. 10, no. 2, pp. 179-195.

Nanwangzi, W & Gan, Y 2017, 'Modelling Thermo-mechanical Behaviour of Geothermal Energy Piles under Cyclic Loading', *Proceedings of the 1st International Conference on Geomechanics and Geoenvironmental Engineering (iCGMGE),* pp. 148-153.

Ng, CWW, Ma, Q & Gunawan, A 2016, 'Horizontal stress change of energy piles subjected to thermal cycles in sand', *Computers and Geotechnics,* vol. 78, pp. 54-61.

Ng, CWW, Shi, C, Gunawan, A & Laloui, L 2014, 'Centrifuge modelling of energy piles subjected to heating and cooling cycles in clay', *Geotechnique letters*, vol. 4, no. 4, pp. 310-316.
Nguyen, VT, Tang, AM & Pereira, J-M 2017, 'Long-term thermo-mechanical behavior of energy pile in dry sand', *Acta Geotechnica*, vol. 12, no. 4, pp. 729-737.
Nguyen, VT; Wu, N; Gan, Y; Pereira, J.M; Tang, A.M 2018, 'Long-term thermo-mechanical behaviour of energy pile in clay', *Environmental Geotechnics*, pp. (in press).
Olgun, CG, Ozudogru, TY, Abdelaziz, SL & Senol, A 2015, 'Long-term performance of heat exchanger piles', *Acta Geotechnica*, vol. 10, no. 5, pp. 553-569.
Park, H, Lee, S-R, Yoon, S & Choi, J-C 2013, 'Evaluation of thermal response and performance of PHC energy pile: Field experiments and numerical simulation', *Applied Energy*, vol. 103, pp. 12-24.
Pasten, C & Santamarina, JC 2014, 'Thermally induced long-term displacement of thermoactive piles', *Journal of Geotechnical and Geoenvironmental Engineering*, vol. 140, no. 5, pp. 06014003.
Saggu, R & Chakraborty, T 2015, 'Cyclic thermo-mechanical analysis of energy piles in sand', *Geotechnical and Geological Engineering*, vol. 33, no. 2, pp. 321-342.
Signorelli, S, Bassetti, S, Pahud, D & Kohl, T 2007, 'Numerical evaluation of thermal response tests', *Geothermics*, vol. 36, no. 2, pp. 141-166.
Stewart, MA & Mccartney, JS 2013, 'Centrifuge modeling of soil-structure interaction in energy foundations', *Journal of Geotechnical and Geoenvironmental Engineering*, vol. 140, no. 4, pp. 04013044.
Suryatriyastuti, M, Mroueh, H & Burlon, S 2014, 'A load transfer approach for studying the cyclic behavior of thermo-active piles', *Computers and Geotechnics*, vol. 55, pp. 378-391.
Tang, A-M, Cui, Y-J & Barnel, N 2008, 'Thermo-mechanical behaviour of a compacted swelling clay', *arXiv preprint arXiv:0802.1433*.
Vieira, A & Maranha, JR 2016, 'Thermoplastic analysis of a thermoactive pile in a normally consolidated clay', *International Journal of Geomechanics*, vol. 17, no. 1, pp. 04016030.
Wehnert, M & Vermeer, P 2004, 'Numerical analyses of load tests on bored piles', *Numerical methods in geomechanics–NUMOG IX*, pp. 505-511.
Xiao, J, Luo, Z, Martin Ii, JR, Gong, W & Wang, L 2016, 'Probabilistic geotechnical analysis of energy piles in granular soils', *Engineering Geology*, vol. 209, pp. 119-127.
Yang, W, Lu, P & Chen, Y 2016, 'Laboratory investigations of the thermal performance of an energy pile with spiral coil ground heat exchanger', *Energy and Buildings*, vol. 128, pp. 491-502.
Yavari, N, Tang, AM, Pereira, J-M & Hassen, G 2014a, 'Experimental study on the mechanical behaviour of a heat exchanger pile using physical modelling', *Acta Geotechnica*, vol. 9, no. 3, pp. 385-398.
Yavari, N, Tang, AM, Pereira, J-M & Hassen, G 2014b, 'A simple method for numerical modelling of energy pile's mechanical behaviour', *Géotechnique Letters*, vol. 4, no. April-June, pp. 119-124.
Yavari, N, Tang, AM, Pereira, J-M & Hassen, G 2016a, 'Effect of temperature on the shear strength of soils and the soil–structure interface', *Canadian Geotechnical Journal*, vol. 53, no. 7, pp. 1186-1194.
Yavari, N, Tang, AM, Pereira, J-M & Hassen, G 2016b, 'Mechanical behaviour of a small-scale energy pile in saturated clay', *Géotechnique*, vol. 66, no. 11, pp. 878-887.
Yoon, S, Lee, S-R, Xue, J, Zosseder, K, Go, G-H & Park, H 2015, 'Evaluation of the thermal efficiency and a cost analysis of different types of ground heat exchangers in energy piles', *Energy Conversion and Management*, vol. 105, pp. 393-402.
You, S, Cheng, X, Guo, H & Yao, Z 2014, 'In-situ experimental study of heat exchange capacity of CFG pile geothermal exchangers', *Energy and Buildings*, vol. 79, pp. 23-31.

Zeng, H, Diao, N & Fang, Z 2002, 'A finite line-source model for boreholes in geothermal heat exchangers', *Heat Transfer—Asian Research: Co-sponsored by the Society of Chemical Engineers of Japan and the Heat Transfer Division of ASME,* vol. 31, no. 7, pp. 558-567.